

# **IMPROVING LIFTING CAPACITY AND MODELLING HYDRAULICS OF LOCAL BASED MUDS FLOWING THROUGH VERTICAL PIPES**

A thesis presented to the Department of Petroleum Engineering African University of Science and  
Technology, Abuja

In partial fulfilment of the requirements for the degree of

**MASTER OF SCIENCE**

By

**ESEIGBE, OSEMUDIAMHEN GODFREY**

Supervised by

Dr. Akeem O. Arinkoola



African University of Science and Technology [www.aust.edu.ng](http://www.aust.edu.ng)

P.M.B 681, Garki, Abuja F.C.T Nigeria

June 2019

## **CERTIFICATION**

We hereby certify that the matter embodied in this thesis entitled "Improving lifting capacity and modelling hydraulics flowing through vertical pipes" has been carried out by Mr Esegbe Osemudiamhen Godfrey, at African University of Science and Technology, Abuja under the supervision of Dr. Akeem O. Arinkoola and that it has not been submitted elsewhere for the award of any degree or diploma.

**IMPROVING LIFTING CAPACITY AND MODELLING HYDRAULICS OF LOCAL BASED MUDS FLOWING THROUGH VERTICAL PIPES**

By

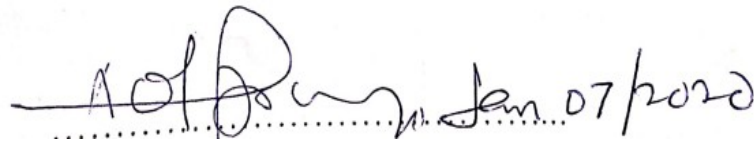
**Eseigbe, Osemudiamhen Godfrey**

A THESIS APPROVED BY THE PETROLEUM ENGINEERING DEPARTMENT



**RECOMMENDED:**.....

**Supervisor;** Dr Akeem O. Arinkoola



.....  
**Head,** Department of Petroleum Engineering

**APPROVED:** .....

**Chief Academic Officer**

.....  
Date

©2019

Eseigbe Osemudiamhen Godfrey

ALL RIGHTS RESERVED

## ABSTRACT

Drilling mud plays an integral part in drilling operations to perform several functions some of which are to cool drill bits, provide hydrostatic pressure and give information about subsurface formation. The cutting suspension and lifting ability of the mud remains one of the most important functions amongst others. Conventional based muds are made of Wyoming bentonite dispersed in water or oil as continuous phase in the presence of synthetic additives to enhance it's property. Previous research showed that Local based muds suffers poor lifting capacity and high pressure loss.

This research work focuses on improving the properties of local based muds with biopolymers and Nanoparticles(Multiwall Carbon nanoparticles and Bamboo raw and Modified) to meet API standards and serve as a substitute to the expensive and environmentally unfriendly synthetic muds and modelling the pressure losses in vertical pipes to observe the effect of nanoparticle addition on pressure loss. Modified Gombe Clay was enhanced with a composite of Gum arabic and Cassava starch, Sodium Hydroxide, Potassium Chloride and weighted with barite to create a base mud formulation. 0.1g, 0.2g, 0.5g and 0.8g MWCNT and BRM were added to create new formulations and rheological readings were taken at room temperature, 60°C and 94°C.

Results showed that at room temperature all CNTs formulation had little or no improvement in gel strengths in comparison with base mud formulation and 0.1g MWCNT formulation amongst other MWCNT and BRM formulations had most favourable gel strength values at 94°C in comparison to base formulation to meet API requirement. Pressure losses of mud flowing in vertical pipes was reduced by 22% and 43% at room temperature and 94°C by the addition of 0.1g MWCNT.

Keywords: Rheology, Lifting Capacity, Gel Strength, Hydraulics, Multiwall Carbon Nanotube, Bamboo Raw and Modified

## **DEDICATION**

This research is dedicated to God almighty for giving me life and health to do this work and surrounding me with persons that add value to my life.

## **ACKNOWLEDGEMENTS**

I am blessed by the kind disposition and support that I received from every staff and student of African University of Science and Technology particularly from the Department of Petroleum Engineering during the entire period of my program.

Special thanks to my supervisors, Dr Akeem Arinkoola, for his commitments and guidance provided towards my academic development. His research lifestyles have taught me to forge ahead and be creative in thinking even when challenges arise.

## TABLE OF CONTENTS

CERTIFICATION.....	i
ABSTRACT.....	iv
DEDICATION.....	v
ACKNOWLEDGEMENTS.....	vi
TABLE OF CONTENTS.....	vii
LIST OF TABLES.....	x
LIST OF FIGURES.....	xi
CHAPTER 1.....	1
INTRODUCTION.....	1
1.1 Background of the study.....	1
1.2 Statement of Problem.....	2
1.3 Aim and Objectives.....	2
1.4 Expected outcomes.....	3
1.5 Facilities to be used.....	3
1.6 Organization of work.....	3
CHAPTER 2.....	4
LITERATURE REVIEW.....	4
2.1 Rheology.....	4
2.1.1 Viscosity.....	4
2.1.2 Yield point and gel strength.....	6
2.1.3 Plastic viscosity.....	6
2.2 Visco-elasticity and thixotropy.....	6
2.3 Thixotropy loop test.....	7
2.4 Time dependent yield stress fluids.....	7
2.5 Rheology in suspensions.....	10
2.5.1 Effect of temperature and aging on drilling muds.....	10
2.5.1 Effects of viscosifiers in water-based drilling muds.....	10
2.5.2 Effects of nanoparticles in water-based drilling muds.....	11
2.6 Local based muds.....	12
2.7 Rheological models.....	12
2.7.1 Bingham plastic model.....	13

2.7.2 Power-law model.....	14
2.7.3 Herschel-bulkley model.....	16
2.7.4 Casson model.....	18
2.7.5 Robertson-stiff model.....	18
2.7.6 Unified model.....	19
2.7.7 Api-model recommended practice 13 d model.....	19
2.8 Hydraulics.....	20
2.8.1 Pressure losses.....	20
2.8.2 Cutting carrying capacity.....	22
2.8.3 Hydraulic models.....	23
CHAPTER 3.....	24
3.1 Materials/equipment.....	24
3.2 Experimental design.....	29
3.2.1 Preparation of blank mud.....	29
3.2.2 Addition of natural viscosifiers.....	29
3.2.3 Addition of nanoparticles.....	30
3.2.4 Rheology and hydraulics.....	30
3.3 Procedures.....	30
3.3.1 Procedure for preparation of mud with and without additive.....	30
3.3.2 Procedure to determine mud density.....	30
3.3.3 Procedure for solid content measurement.....	31
3.3.4 Procedure to determine rheology using 8-speed viscometer.....	31
3.3.5 Procedure to determine gel strength using 8-speed viscometer.....	32
3.3.6 Calculations for rheology and API standards.....	32
CHAPTER 4.....	34
4.1 SEM and EDS characterisation of materials.....	34
4.2 Rheology.....	38
4.2.1 Effect of temperature on rheology of base weighted mud formulation.....	45
4.2.2 Effect of nanoparticles on rheology of base weighted mud formulations..	47
4.3 Rheological models.....	54
4.4 Frictional Pressure Losses model estimation.....	62
CHAPTER 5.....	65
CONCLUSION AND RECOMMENDATION.....	65
5.1 Conclusion.....	65

5.2 Recommendations..... 65

**LIST OF TABLES**

Table 3.1: Components of drilling mud formulations..... 29

Table 3.2: API standards for drilling fluid properties.....	34
Table 4.1: Property values of mud formulations without additives.....	39
Table 4.2: Mud Formulations with additives.....	40
Table 4.3: Weighted and Unweighted mud formulations at room temperature.....	44
Table 4.4: Rheological properties of weighted and unweighted mud formulations at room temperature in comparison to API standard.....	45
Table 4.5: Types and concentrations of materials used in the formulated weighted drilling muds.....	46
Table 4.6: Effects of MWCNT on drilling mud.....	49
Table 4.7: Effects of BRM on drilling mud.....	50
Table 4.8: Pressure loss model data for base case and MWCNT formulations at 26.5°C.....	65
Table 4.9: Pressure loss model data for base case and MWCNT formulations at 94°C.....	66

## LIST OF FIGURES

Figure 2.1: Shear stress vs Shear rate for a Newtonian fluid (Adam el al 1986).....	5
---	---

Figure 2.2: shear stress vs shear rate (a) Pseudo plastic behaviour (b) Dilatant behaviour (Adam et al 1986).....	6
Figure 2.3: shear stress vs time (a) Thixotropic behavior (b) Rheopetic behavior (Adam et al,1986).....	6
Figure 2.4: Thixotropy loop test plot of shear stress versus shear rate (American concrete institute, 2014).....	8
Figure 2.5: Distinguishing time-dependence from viscoelasticity .Shear rate response to a step shear stress increase (a) Imposed step-change in shear stress (b) Time-independent viscoelastic fluids (c) Time-dependent viscous inelastic fluids (d) Time-dependent viscoelastic fluids (de Souza Mendes & Thompson, 2019).....	10
Figure 2.6: Distinguishing time-dependence from viscoelasticity. Viscosity response to a step shear stress increase (a) Imposed step-change in shear stress (b) Time-independent viscoelastic fluids (c) Time-dependent viscous inelastic fluids (d) Time-dependent viscoelastic fluids(de Souza Mendes & Thompson, 2019).....	11
Figure 2.7:MWCNTs ,POCNTs and addition of POCNTs with clay platelets (Kazemi-Beydokhti & Hajiabadi, 2018).....	12
Figure 2.8:Shear stress versus shear rate behaviour for Bingham plastics (Adam et al,1986).....	15
Figure 2.9: Power law fluids shear stress and shear rate relationship for (a) Pseudoplastics (b) Dilatants (Adam et al,1986).....	16
Figure 2.10 : Log-Log plot of Power law model (Bahrainian et al., 2018).....	17
Figure 2.11: Herschel-Buckley fluid rheological behaviour (Slumberger Oilfield Glossary).....	18
Figure 2.12 : Log-Log graph of Herschel-Bulkley model (Bahrainian et al., 2018).....	18
Figure 2.13: Graphical Representation of Casson model (Hossain, 2016).....	19
Figure 2-14: Newtonian and Non-Newtonian fluids (Nguyen & Nguye, 2012).....	21
Figure 3.1: ZEISS SEM Equipment for SEM AND EDS Characterisation.....	26
Figure 3.2: Weighing Balance.....	27
Figure 3.3: Sand content kit.....	27
Figure 3.4: Ofite Multi-mixer.....	28
Figure 3.5: Ofite Mud Balance.....	28
Figure 3.6: Ofite 8 speed viscometer model 800.....	29
Figure 3.7:(a) Gum arabic sample (b) Corn Starch sample (c) Cassava Starch sample (d)Modified Gombe clay sample (e) Barite sample.....	30
Figure 3.8: Experimental design.....	30
Figure 3.9(a): Modified Gombe based Mud Samples (b)Bamboo Raw but modified carbon nanoparticles (BRM) (c) Multiwall carbon nanotubes(MWCNT).....	31
Figure 4.1: SEM Images of sample X1 at resolutions of 100 $\mu\text{m}$ .....	35
Figure 4.2: SEM images of sample X2 at resolutions of (a) 10 $\mu\text{m}$ (b) 20 $\mu\text{m}$ .....	36
Figure 4.3: SEM Images of sample X3 at resolutions of (a) 20 $\mu\text{m}$ (b) 200 $\mu\text{m}$ .....	37
Figure 4.4: SEM Images of sample X4 at resolution of 100 $\mu\text{m}$ .....	37
Figure 4-5: SEM Images of sample X5 at resolution of 100 $\mu\text{m}$ .....	37
Figure 4.6: SEM Images of sample X5 at resolution of 100 $\mu\text{m}$ .....	38
Figure 4-7: XRD showing Mineralogy of treated and untreated clay.....	39
Figure 4.8: Chart showing rheological properties of mud before and after addition of corn starch at various concentration.....	42
Figure 4.9: Chart showing rheological properties of muds before and after addition of gum arabic of various concentration.....	43
Figure 4.10: Comparison between Cassava starch, Gum Arabic and Corn starch 600rpm and gel behavior in mud.....	44

Figure 4.11: Comparison between rheology of weighted and unweighted 20g cassava starch and 20g gum arabic mud formulations.....	46
Figure 4.12: Plastic viscosity against temperature for base weighted mud formulation.....	48
Figure 4.13: Yield Point versus Temperature for base weighted mud formulation.....	48
Figure 4.14: Gel strength versus temperature for base weighted mud formulation.....	49
Figure 4.15: Effect of MWCNT and BRM on 10 seconds gel at 26.64°C.....	51
Figure 4.16: Effect of MWCNT and BRM on 10 minutes gel at 26.64°C.....	52
Figure 4.17: Effect of MWCNT and BRM on 10 seconds gel at 60°C.....	52
Figure 4.18: Effect of MWCNT and BRM on 10 minutes gel at 60°C.....	53
Figure 4.19: Effect of MWCNT and BRM on 10 seconds gel at 94°C.....	53
Figure 4.20: Effect of MWCNT and BRM on 10 minutes gel at 94°C.....	54
Figure 4.21: Effect of 0.1g, 0.2g, 0.5g and 0.8g concentrations of MWCNT and BRM on 10 seconds gel at different temperatures.....	55
Figure 4.22: Effect of 0.1g, 0.2g, 0.5g and 0.8g concentrations of MWCNT and BRM on 10 minutes gel at different temperatures.....	55
Figure 4.23: Effect of 0.1g, 0.2g, 0.5g and 0.8g concentrations of MWCNT and BRM on Plastic viscosity at different temperatures.....	56
Figure 4.24: Effect of 0.1g, 0.2g, 0.5g and 0.8g concentrations of MWCNT and BRM on yield point at different temperatures.....	57
Figure 4.25: Consistency plot for 0.1g MWCNT and 0.1g BRM at 26°C.....	58
Figure 4.26: Consistency plot for 0.1gMWCNT and 0.1gBRM at 60°C.....	58
Figure 4.27: Consistency plot for 0.1gMWCNT and 0.1gBRM at 94°C.....	59
Figure 4.28: Bingham model for Weighted (base)mud rheology plot at 25°C.....	59
Figure 4.29: Power law model for Weighted (base)mud rheology plot at 25°C.....	60
Figure 4.30: Herschel Bulkley model for Weighted (base)mud rheology plot at 25°C.....	60
Figure 4.31: Bingham model for Weighted (base)mud rheology plot at 94°C.....	61
Figure 4.32: Power law model for Weighted (base) mud rheology plot at 94°C.....	61
Figure 4.33: Herschel Bulkley model for Weighted (base)mud rheology plot at 94°C.....	62
Figure 4.34: Bingham model for MWCNT mud rheology plot at 26.5°C.....	62
Figure 4.35: Power law model for MWCNT mud rheology plot at 26.5°C.....	63
Figure 4.36: Herschel Bulkley model for MWCNT mud rheology plot at 26.5°C.....	63
Figure 4.37: Bingham model for MWCNT mud rheology plot at 94°C.....	64
Figure 4.38: Power law model for MWCNT mud rheology plot at 94°C.....	64
Figure 4.39: Herschel Bulkley model for MWCNT mud rheology plot at 94°C.....	65
Figure 4.40: Pressure loss profile at 26.5°C for base and 0.1g MWCNT mud formulations.....	67
Figure 4.41: Pressure loss profile at 94°C for base and 0.1g MWCNT mud formulations.....	67

# CHAPTER 1

## INTRODUCTION

### 1.1 Background of the study

The carrying capacity of drilling fluid is a measure of its effective capability to transport cuttings to the surface. Cuttings transportation depends on mud rheology and other factors such as wellbore inclination, flow regime, slip velocity, drill pipe revolution, flow rate, rate of penetration, cuttings size and shape, wellbore geometry and other drilling parameters. Rheological properties of drilling fluids are important for evaluating drilling fluid behavior to solve problems of hole cleaning and hole erosion, suspension of cuttings, drilling fluid treatment, and hydraulics calculations. Optimizing drilling fluid parameters is important to achieve a successful drilling process.

Density and viscosity of drilling fluid are designed so that they provide the best pressure control and hole cleaning. The drilling fluid properties change depending on its state (dynamic and steady), and therefore presents big challenges to designing a drilling fluid that exhibits adequate qualities both at rest and in motion. When the pumps are shut off or operating at relatively low speed the drilling fluid assumes a gel-like state. The gelling of the drilling fluid is vital in keeping drill cuttings and barite in suspension in the drilling fluid. It is not desired to allow cuttings and other solids to settle in the wellbore. To achieve this, it is desirable that the drilling fluid quickly develops relatively high gel strength. However, an excessive gel is not desirable but it is expected that when the gel developed to required strength the strength stays at this level as time goes, and that it does not continue to grow further. This is important because increased energy is required to break the gel and resume circulation. This leads to a pressure peak in the borehole, and this peak mustn't exceed the fracturing pressure of the formation.

Drilling fluids are divided into two different categories depending on their content. Because water-based mud (WBM) is the most common drilling fluid for both offshore and onshore areas, water-soluble polymers (WSPs) are preferred in drilling fluids. Water-based drilling fluids consist mainly of water and clay and are considered a suspension. Oil-based drilling fluids consist mainly of base oil and water emulsion. A range of additives is also added to influence properties such as density, viscosity, and wettability. Synthetic polymers react with calcium and

exhibit severe viscosity and gelation (Bloys et al., 1994). Synthetic polymers are expensive and generally salt- and pH-sensitive, compared to natural polymers.

Natural polymers rely on chain extension and physical entanglement of solvated chains for viscosity enhancement. They are non-charged and less sensitive to salts in contrast to the synthetic ones (Annis, and Smith, 1974). Examples of natural polymers include starch, carboxymethyl cellulose (CMC), and Hydroxyethylcellulose (HEC). Some hemicelluloses, such as mannans (guar gum, locust bean gum, and konjac glucomannan), have been utilized for a long time due to their nontoxicity, solubility in water, and ability to form gels (Baba Hamed and Belhadri, 2009). Examples of gums include exudate (Arabic, karaya), microbial fermentation (pullulan, xanthan gum, dextran, and gellan gum), and seed gums (guar gum) (Teleman et al., 2003).

Drilling fluids experience an extreme range of different external conditions such as temperatures, pressures, and shear rates. Extensive testing is therefore required for prediction of behaviour and to generate accurate models before these polymers are deployed on the field.

## **1.2 Statement of Problem**

The application of local clays and additives at field level has not been widely reported. This is due to certain inherent property limitations when compared with the API requirements. Studies (Arinkoola et al., 2017, 2018) have shown the potential of local biopolymers and clay in oil and gas. The hydraulics of bentonite and other local additives dispersed in water are not widely reported. Research (Atitebi et al., 2018) has shown that the use of 100% local materials in the formulation of drilling mud suffers poor lifting capacity, high-pressure loss and thermal instability due to altered rheological properties at downhole conditions. Hence, this study intends to improve on cuttings carry ability and thermal stability of local-based mud using synthetic multi-walls carbon nanotubes (MWCNTs) and locally sourced Activated carbon (BRM) produced from a Bamboo tree.

## **1.3 Aim and Objectives**

This study aim at improving the cuttings carrying capacity and thermal stability of local-based mud using MWCNTs and Activated carbon produced from Bamboo (BRM). Objectives are

1. Characterization of beneficiated local clay and additives using SEM and EDS

2. Sensitivity study on the effect of biopolymers on mud's Shear stress at 600 RPM and Gel at 10' and 10"
3. Determination of the effect of BRM and MWCNT on the Gel at 10' and 10" and determination of the optimum amount of carbon for effective mud formulation.
4. Determination of the appropriate rheological model for the weighted mud based on the result obtained from (3) above.
- 5 Frictional pressure loss modelling using rheological parameters obtained from (4).

#### **1.4 Expected outcomes**

It is expected that at the end of this work the following shall be achieved:

- Creation of locally-based muds having rheological properties that befit API standard.
- Enhancement of lifting capacity of the created local based to meet API standard.

#### **1.5 Facilities used**

The facilities and resources for this project include;

- AUST library and internet facilities
- AUST laboratory

#### **1.6 Organization of work**

This report is organized into five chapters. Chapter one is the introductory chapter giving general information about the entire project. Chapter two gives in-depth information on the reviews of relevant literature related to this work. Chapter three places emphasis on experimentation and methodology. Chapter four covers the results and discussion. The last chapter which is chapter five concludes the project and provides the necessary recommendations.

## Chapter 1

### LITERATURE REVIEW

#### 2.1 Rheology

Rheology is a science that deals with the study of the flow behaviour of suspension in pipes and conduits and the relationship between flow pressure and flowrates, shear stress and shear rate (Caenn, Darley, & Gray, 2016). Drilling fluid functions include formation pressures control, hole integrity and stability maintenance, lubricating and cooling of the drill bit, and drill string, bottom hole cleaning, suspension of cuttings in the annulus when circulation is stopped and carrying them to the surface during drilling. The rheological behavior of a drilling fluid directly affects all these activities and enables better estimation of flow regimes, frictional pressure losses, equivalent circulating and surge and swab pressure which promotes hole cleaning efficiency (Guo & Liu, 2011). Rheological properties of drilling mud affect the ability of the mud to perform its functions and its knowledge is useful in the design and evaluation of rig circulating systems and hydraulics (Sadek et. Al,2011; Gowariker et.al, 1995). Rheology of drilling mud is characterized by viscosity, yield point, and gel strength.

##### 2.1.1 Viscosity

Shlumberger Oilfield Glossary defines viscosity as a measure of the ability of fluids to resist flow. It is expressed mathematically as the ratio of shear stress to shear rate. Mathematically, for Newtonian fluid, it is the ratio of shear stress to shear rate as shown in figure 2.1.

$$\text{viscosity } \mu = \frac{\text{Shear stress, } \tau}{\text{Shear rate, } \dot{\gamma}} \quad \text{Equation 2.1}$$

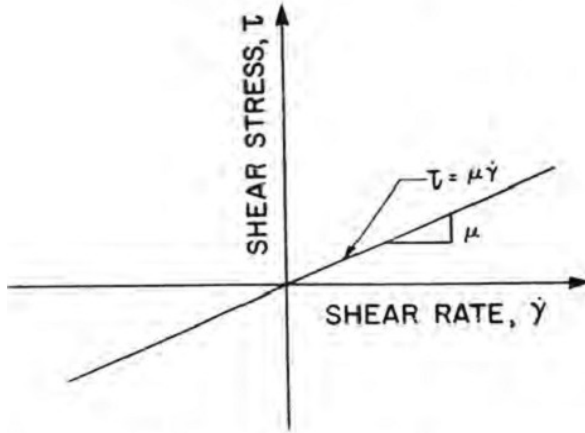


Figure 2.1: Shear stress vs Shear rate for a Newtonian fluid (Adam et al 1986)

Adam et al,(1986) stated that drilling fluids are non-newtonian and don't exhibit direct shear stress and shear rate relationship and hence, exhibit no single viscosity value at various shear rates. Non-newtonian fluids could be shear rate or shear-time dependent. Non-newtonian fluids whose apparent viscosity reduces with increasing shear rates are called pseudoplastic (fig 2.2a) and dilatant (fig 2.2b) if apparent viscosity increases with increasing shear rate. Shear-time dependent non-newtonian fluids are thixotropic (fig 2.3a) if apparent viscosity decreases as the shear rate is increased to a new value that is constant. It is rheopetic (fig 2.3b) if the apparent viscosity increases with time after the shear rate is increased to a new constant value. Drilling fluid generally is pseudoplastic and thixotropic.

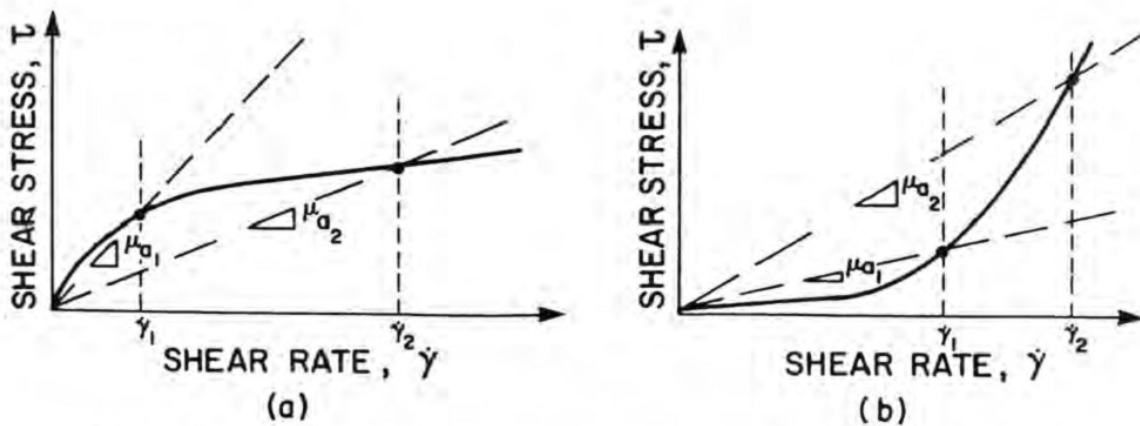


Figure 2.2: shear stress vs shear rate (a) Pseudo plastic behaviour (b) Dilatant behaviour (Adam et al 1986)

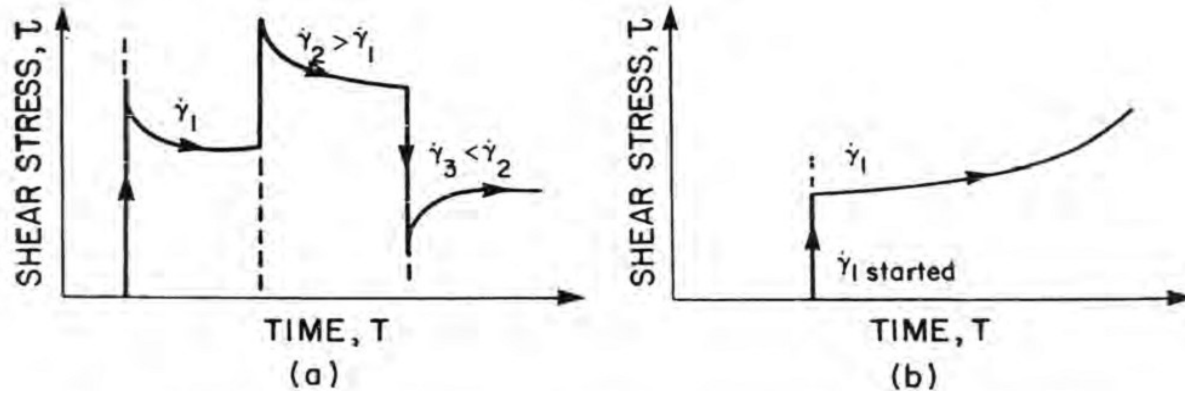


Figure 2.3: shear stress vs time (a) Thixotropic behavior (b) Rheopetic behavior (Adam et al,1986)

### 2.1.2 Yield point and gel strength

According to (Halliburton, 2007), it had been observed that drilling fluids will only flow when subjected to certain load stress called yield stress. (Sadek et al,2011) explains yield point as the resistance to initial flow or the stress required to start fluid movement caused by electrical charges located or close to the surface of the particles in the mud. Gel strength is a function of inter-particle forces of drilling mud and the shear stress measured at a low shear rate (Nagham Amer Sami,2015). Gel strength is related to yield stress because it is a measure of the same inter-particle forces of a fluid as determined by the yield value except that it is measured under static condition. Effective solids control affects the ability to maintain gel strength within some specified range. Gel strength helps in the suspension of drilled cuttings when circulation is stopped (Sadek et al,2011).

### 2.1.3 Plastic viscosity

The measure of the internal resistance to fluid flow due to the amount, type and size of solids present in a given fluid is called plastic viscosity. Plastic viscosity is increased when there is accumulations of drilled solids, additions of barite, and presence of chemical contaminants and decreased when drilling mud is diluted with water, there is an effective use of solids control equipment and flow line flocculation to remove fine size solids (Sadek et al, 2011).

## 2.2 Visco-elasticity and thixotropy

Viscoelastic fluids are fluids that exhibit viscous and elastic behavior. They could be linear or non-linear. Linear visco-elastics is time dependence fluid since their microstructure takes time to

respond to stress. The elastic behavior of such fluids is seen when the fluid is strained for a short time and the fluid returns to its original structure because it does not respond to the stress applied. The viscous nature of such fluid is seen during a long time strain period as the structure of the fluid adjusts itself continuously that is, the fluid flows and its viscous nature is seen. Non-linear viscoelastic also exhibits time dependence but the microstructure is broken down as it responds to stress after a long time. The microstructure responds to stress after a long period and is changed by the flow. This continuous deformation is called shear thinning as seen in the concept called Thixotropy. Hence, Thixotropic fluids are non-linear viscoelastic fluids or inelastic fluids with shear thinning characteristics. The shear-thinning occurs when rod-like particles align themselves in a flow direction, there is a breakdown of flocs or rearrangement of microstructure in suspensions(Barnes,1996)

### **2.3 Thixotropy loop test**

Halliburton, (2007) evaluated the thixotropic behaviour of four drilling fluids at the temperature of 120 °F. Thixotropy loop test was performed with a Model 35A Viscometer. Four drilling muds were initially pre-sheared at  $1022 \text{ s}^{-1}$  for two minutes to break its structures and allowed to rest for either 10 seconds or 10 minutes for the structure to rebuild and afterwards, the mud is sheared from  $0 \text{ s}^{-1}$  to  $100 \text{ s}^{-1}$  to give an up shear curve and swept back to  $0 \text{ s}^{-1}$  to give a down shear curve in a shear stress versus shear rate plot. He classified thixotropy as either positive thixotropy if the structure recovers during the rest period after pre-shear and is broken down upon shearing. This is evident when up curve runs above the down shear curve. If the structure refuses to be recovered upon resting after pre-sheared, reverse loop is generated due to a shear-induced increase viscosity caused by the application of a high shear rate and the downward curve is above the up shear curve.

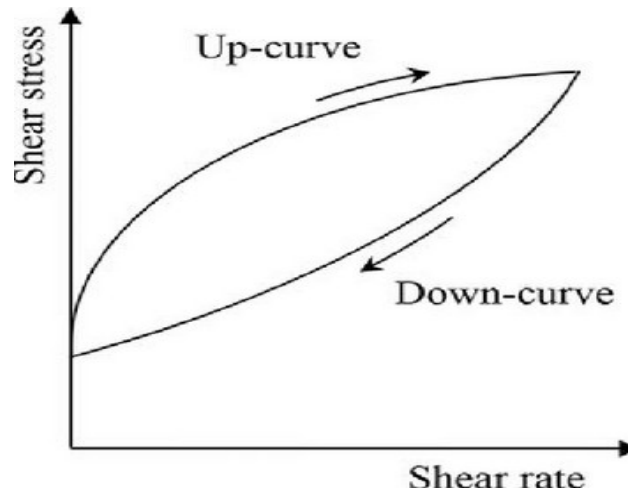


Figure 2.4: Thixotropy loop test plot of shear stress versus shear rate (American concrete institute, 2014)

#### 2.4 Time dependent yield stress fluids

de Souza Mendes & Thompson, (2019) defined time-dependent fluids as fluids whose viscosity change is dependent on the time of shear. These changes are due to their structural level of microstructure. Time-dependent fluid could be reversible or irreversible. The viscosity of reversible time-dependent fluids is not a function of shear history. They have a single unique flow curve. Fluid with varying property is irreversibly time-dependent. Reversible time-dependent fluids could be thixotropic or anti-thixotropic or rheopectic. Thixotropic fluids exhibit shear-thinning property and their viscosity decreases continuously with time as shear stress is increased by a step and vice versa. Rheopectic fluid exhibit shear thickening property as their viscosity increases continuously with time with a step increase in shear stress. Time-dependent fluids differ from a viscoelastic liquid in that viscosity changes in viscoelastic fluids are due to the storage of elastic energy and energy recovery within the microstructure of the energy of the liquids. Time dependent viscoelastic fluids combine the effect of time dependence and viscoelasticity.

Four shear rate step test and plots of shear stress versus time, shear rate versus time and viscosity versus time were used to describe the difference between time dependence and viscoelasticity. The plot in fig 2.5(a) and fig 2.6(a) shows that the sample was exposed to constant stress  $\sigma_i$  initially for a long period of time and then at some time  $t = 0$ , the stress suddenly increased and remained constant for some stress  $\sigma_f$ . fig 2.5b and 2.6b show Jeffreys

viscoelastic liquid of relaxation viscosity  $\eta_1$ , retardation viscosity  $\eta_2$  and shear modulus  $G$ . At  $t < 0$  flow is in equilibrium and steady, At  $t = 0$ , shear stress increases causing a continuous increase in shear rate until another steady state is achieved. Hence, the shear rate is a continuous function at  $t = 0$  but viscosity is discontinuous as there is a viscosity jump at  $t=0$  and then a decrease until a steady state is achieved. fig 2.5c and 2.6c show a purely viscous or time-dependent fluid. At  $t < 0$ , the low shear stress causes a high equilibrium structural level of microstructure and a low shear rate which is in equilibrium. As the shear stress and rate increases, immediately the microstructure begins to breakdown. This continues as shear rate increases monotonically under high shear stress and reach an equilibrium. Viscosity on the other hand, decreases monotonically by the action of high shear stress until equilibrium viscosity is reached at some large enough time. Shear rate after  $t = 0$  is discontinuous while viscosity is continuous. This is the behaviour of an inelastic yield stress shear-thinning time independent fluid. Fig 2.5d and fig2.6d show the behavior of a viscoelastic time-dependent fluid which is opposite to that of fig 2.5c and 2.6d. Most time-dependent fluids possess viscoelastic property and depicts the behavior shown in fig 2.5d and fig 2.6d.

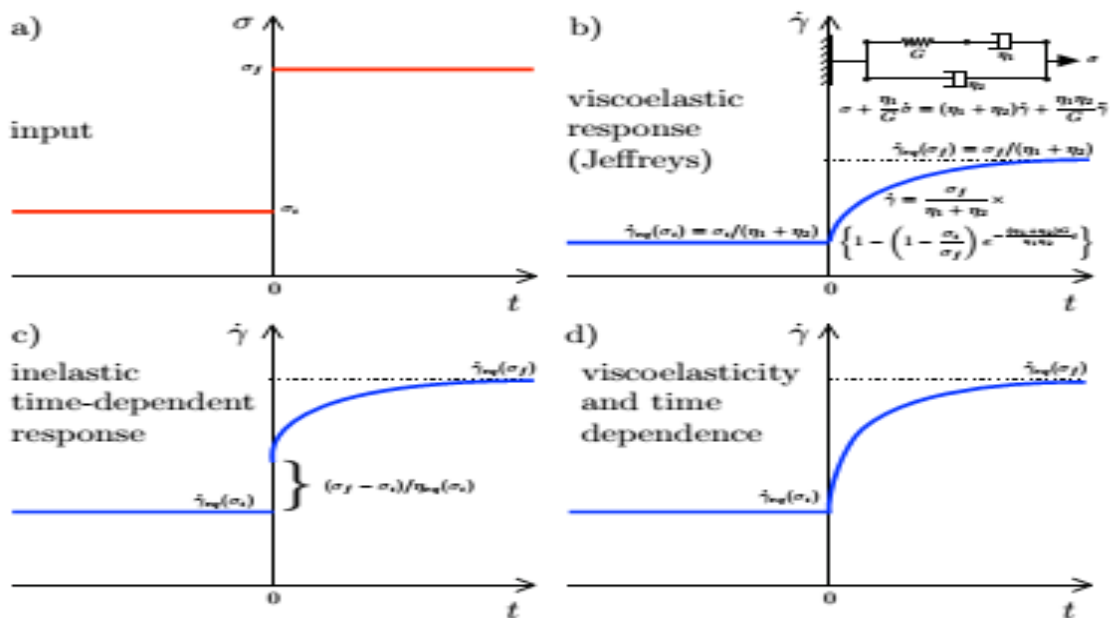


Figure 2.5: Distinguishing time-dependence from viscoelasticity .Shear rate response to a step shear stress increase (a) Imposed step-change in shear stress (b) Time-independent viscoelastic

fluids (c) Time-dependent viscous inelastic fluids (d) Time-dependent viscoelastic fluids (de Souza Mendes & Thompson, 2019)

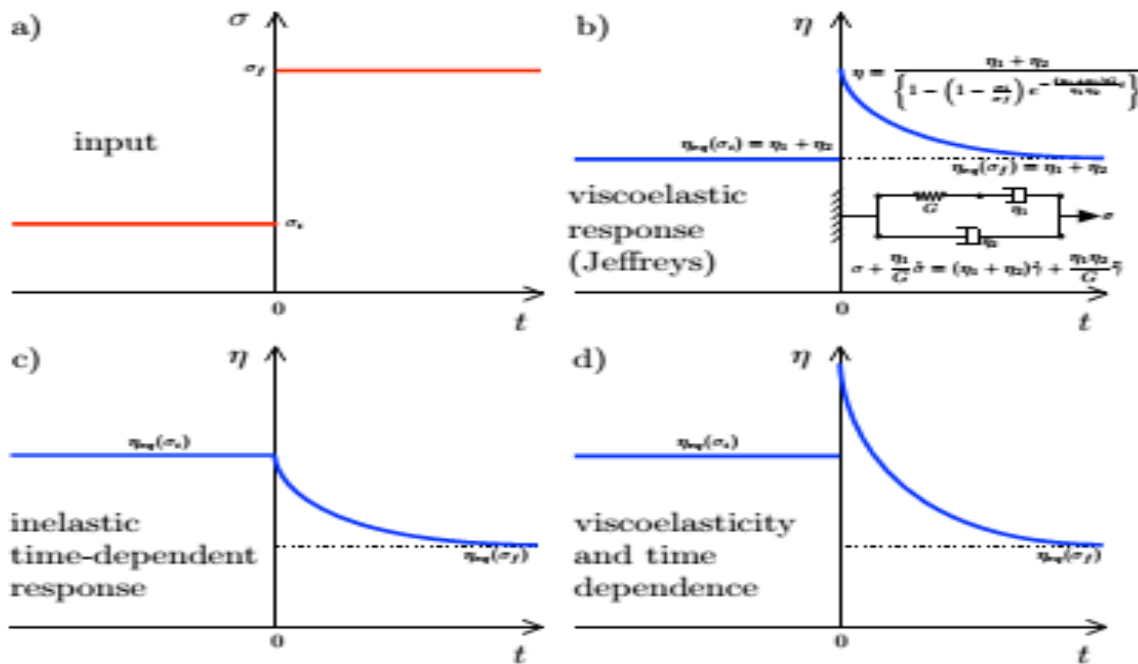


Figure 2.6: Distinguishing time-dependence from viscoelasticity. Viscosity response to a step shear stress increase (a) Imposed step-change in shear stress (b) Time-independent viscoelastic fluids (c) Time-dependent viscous inelastic fluids (d) Time-dependent viscoelastic fluids(de Souza Mendes & Thompson, 2019)

## 2.5 Rheology in suspensions

Conventional drilling muds are suspensions of Wyoming bentonite clay and chemicals in a continuous oil or water phase (Adam et al,1986). Various researches have been done in various mud suspension or mixtures to study rheological behaviour of muds under different conditions of temperature, aging, and presence of additives.

### 2.5.1 Effect of temperature and aging on drilling muds

Olise, Ekaette, & Okologume, (2017) in their work showed the effect of aging on drilling mud suspension. They prepared a bentonite water-based mud weighted with barite and left it for 1,3,5,7 days respectively while increasing the temperature from 37°C to 50°C to 100°C and 150°C, successively. It was observed that viscosity and filtrate loss decreased as density and sand content increased with aging and temperature. (Sami, 2016) also observed a decline in plastic

viscosity for lignite and gypsum muds at an increase in temperature from 80.6°F to 100°F due to thermal degradation.

### **2.5.1 Effects of viscosifiers in water-based drilling muds**

Additives are used in drilling muds to improve rheological and filtration features which in turn aid drilling mud functions. Excessive fluid loss and low gel strength are common challenges that require attention (Akeem Olatunde Arinkoola, Olalekan, Salam, Omolola, & Gafar, 2018). Polymers like Carboxymethylcellulose, hydrolyzed polyacrylate, welan gum are added to drilling muds to boost their viscosity and control filtration (Akeem Olatunde Arinkoola et al., 2018). (Taiwo, Joel, & Kazeem, 2011) showed the potential of local Cassava starch flour in various concentrations to increase viscosity and reduce filtration loss in bentonite drilling muds by 8%. Corn starch as well in (Ghazali, Alias, Mohd, Adeib, & Noorsuhana, 2015), when added in various concentrations (0 to 10 g), caused an increment in viscosity and gel strength and decrease infiltrate loss. (Alflah, Balola, Ibrahim, & Wagialla, 2015) tested the effect of Al-Taleh, Al-Dama zene and Abu Jabiahe Gum Arabic samples in water-based muds and observed an increase in apparent and plastic viscosity for low-temperature ranges and stability between 50°C to 80°C. It decreased at higher temperatures. Yield points and gel strength increased between 30°C to 50°C. Gel strength was unstable between 50°C to 80°C and was stable at a higher temperature. Filtration loss increased between 30°C to 50°C, was semi-stable between 50°C to 80°C and decreased between 80°C to 100°C.

### **2.5.2 Effects of nanoparticles in water-based drilling muds**

Gbadamosi et al., (2018) studied the effects of nano-silica, SiO<sub>2</sub> on drilling muds rheological properties and cutting transport using a flow loop experiment. The authors observed an increase in viscosity, yield point and gel strength with a decrease in filtrate loss which guaranteed mud stability. Higher concentrations of SiO<sub>2</sub> produced higher cuttings recovery for small size cuttings and lowest for large size cuttings. Kazemi-Beydokhti & Hajiabadi, (2018) investigated the effects of multi-walled carbon nanotubes (MWCNTs) wrapped with polyethylene glycol (POCNT) on water-based muds and observed an increase in viscosity and yield stress with a decrease in fluid loss up to 82% by volume as POCNT concentrations increases. These observations were attributed to the large surface area to volume ratio of POCNT when compared to the clay particles in the muds. The interaction and friction in the solution resulted

in the increased viscosity observed. The figure 2.7 shows the structure of multi-walled carbon nanotubes before and after grafting with polyethylene glycol (PEG) and the effect of POCNT with clay platelets.

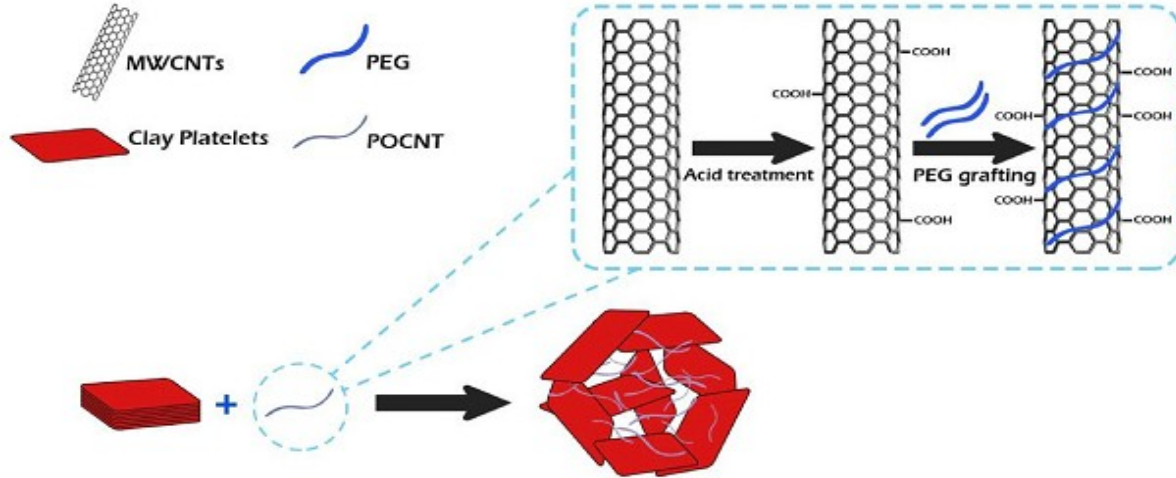


Figure 2.7: MWCNTs, POCNTs and addition of POCNTs with clay platelets (Kazemi-Beydokhti & Hajiabadi, 2018)

## 2.6 Local based muds

Few researches have been reported focusing on bentonite based muds with local additives. Although, oil-based muds are costly and environmentally hazardous than Water-based muds, additives used in water-based particularly the synthetic based ones are also expensive. Consequently, the need for drilling mud cost optimization using indigenous additives is necessary (Ogunmola, Arinkoola, Salam, Jimoh, & Salawudeen, 2017). Arinkoola et al., (2017, 2018) in their work discovered a huge potential of local biopolymers and clay in oil and gas for improve rheology and filtration properties. The hydraulics of bentonite and other local additives dispersed in water is not widely reported. Atitebi et al., (2018) have shown that the use of 100% local materials in the formulation of drilling mud suffers poor lifting capacity, high pressure loss and thermal instability due to altered rheological properties at downhole conditions. Hence, this research work intends to improve cutting carrying ability and thermal stability in local based muds using synthetic and locally produced mul-tiwall carbon-nanotubes.

## 2.7 Rheological models

Bahrainian, Nabati, & Hajidavalloo, (2018) defined rheological model as mathematical equations used to predict fluid behaviour across wide range of shear rate. Adam et al, (1986) stated that rheological models are used by engineers to approximate fluid behavior. These equations are required for the description of viscous forces present in the liquid which is required in calculation of frictional losses in Hydraulics. Various rheological models have been developed to explain the behavior of fluids. Basically there are two models namely;

- Newtonian model
- Non-newtonian model

Newtonian models are used for fluid with constant or single viscosity which is measured by the slope of the line in figure 2.1. Shear stress exhibited by such fluids is proportional to shear rate. Example of such fluids are water and gases. The Newtonian model is expressed mathematically as

$$\tau = \mu \dot{\gamma} \quad \text{Equation 2.2}$$

Where  $\tau$  = Shear stress in dyne per square centimeter

$\mu$  = Viscosity in centipoise

$\dot{\gamma}$  = Shear rate in per seconds

Non-newtonian models are used model which characterise fluids that do not have a direct proportionality shear stress shear rate relationship. (Bahrainian et al., 2018) in their work characterised an oil based drilling fluid for south western Iranian oilfield using five non-newtonian model namely:

- Bingham Plastic model
- Power law model
- Herschel-Bulkley model
- Casson model
- Robertson Stiff model.

### 2.7.1 Bingham plastic model

Bingham plastics are described by two-parameter which are plastic viscosity and yield point and exhibit linear shear stress and shear rate ratio after specific shear stress is exceeded (Bahrainian et al., 2018). Bingham plastics will not flow until the shear stress applied exceed some certain minimum value called yield point denoted by  $\tau_y$ . changes in shear stress to shear rate is proportionally constant after the yield point. This constant is called plastic viscosity and is denoted as  $\mu_p$ . Shear stress at zero shear rate is called the yield point(Bahrainian et al., 2018). According to Schlumberger Oilfield glossary, yield point must be high enough to ensure cuttings are suspended and carried to the surface but not too high as to create excessive pump pressure during drilling operations. Plastic viscosity should be low by ensuring fewer solids or colloids are present in the drilling mud to ensure good lifting capacity of cuttings downhole. Bingham plastic model is a linear model that does not describe fluids at low shear rate regions((Guo & Liu, 2011). (Adam et al,1986) presented mathematical expressions and graphical representation of Bingham plastics given in Equation 2.3 and 2.4 and figure 2.6

$$\tau = \mu_p \dot{\gamma} + \tau_y ; \tau > \tau_y \quad \text{Equation 2.3}$$

When  $\dot{\gamma}=0$ ,  $-\tau_y \leq \tau \leq +\tau_y$  and

$$\tau = \mu_p \dot{\gamma} - \tau_y ; \tau < -\tau_y \quad \text{Equation 2.4}$$

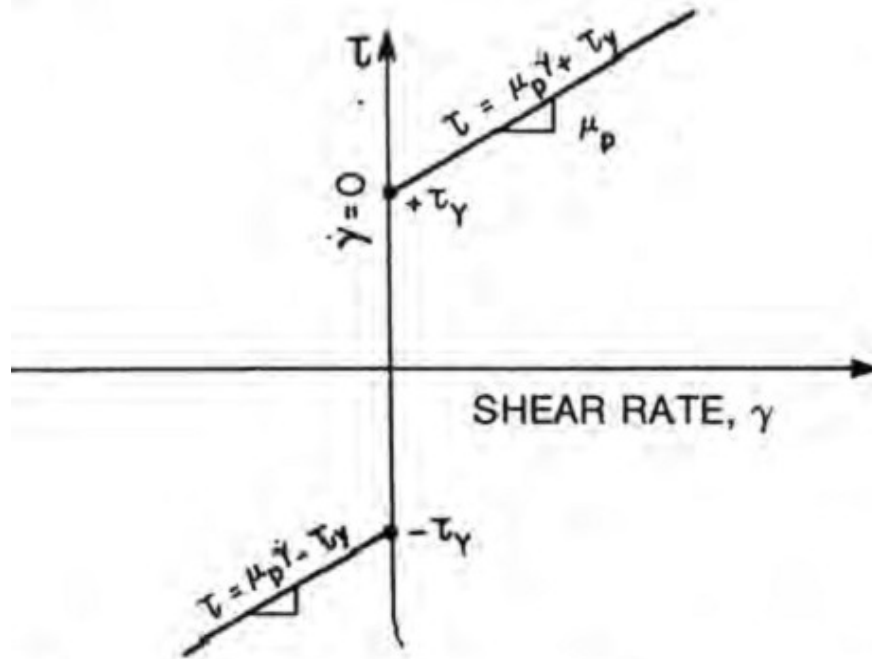


Figure 2.8: Shear stress versus shear rate behaviour for Bingham plastics (Adam et al, 1986)

### 2.7.2 Power-law model

The power-law model also requires two parameters for the characterization of fluids. It can be used to represent a pseudo-plastic fluid, a Newtonian fluid or a dilatant fluid. It is defined by the expression

$$\tau = K|\dot{\gamma}|^{n-1}\dot{\gamma} \quad \text{Equation 2.5}$$

Where  $k$  is the consistency index of the fluid and  $n$  is the flow behavior or power-law exponent (Adam et al, 1986). According to Bahrainian et al., (2018),  $n$  measures the degree of non-newtonian behavior and  $k$  measures the consistency of the fluid. The higher the  $k$  value, the more viscous the fluid becomes. Adam et al, (1986) also stated that when  $n=1$ , the fluid is Newtonian,  $n<1$  typifies a pseudoplastic fluid and when  $n>1$ , the represents a dilatant fluid. The figures below show power-law fluids for pseudoplastic and dilatant.

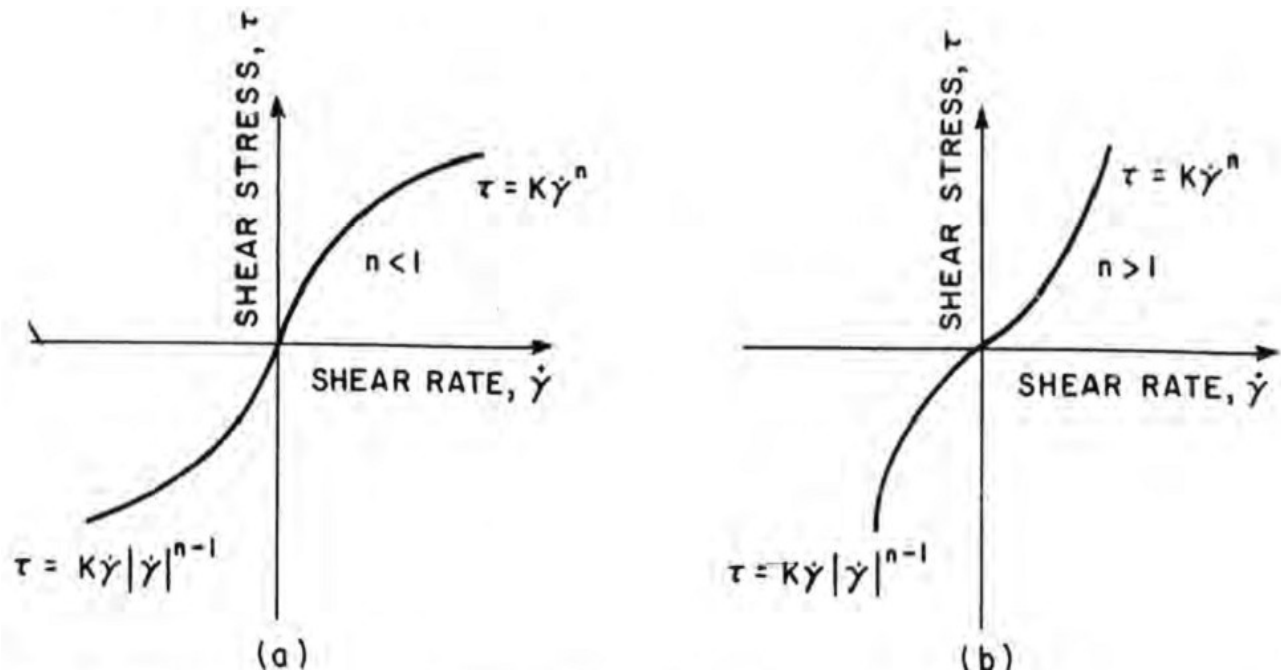


Figure 2.9: Power law fluids shear stress and shear rate relationship for (a) Pseudoplastics (b) Dilatants (Adam et al,1986)

Bahrainian et al., (2018) stated that true power law fluids model has no yield stress (intercept) and showed how power law fluids can be plotted in a log-log plot to determine flow behavior and consistency of the fluids .The log of shear stress when plotted to that of shear rate gives a straight line which has an intercept the log of shear stress at zero shear rate. Taking the log of both sides of Equation 2.5 gives Equation 2.6.

$$\text{Log}\tau = \text{Log} k + n \text{Log} \dot{\gamma} \quad \text{Equation 2.6}$$

Where flow behavior n is the is the slope of the plot and is given as

$$\text{Slope } n = \frac{\text{Log}\tau_2 - \text{Log}\tau_1}{\text{Log}\dot{\gamma}_2 - \text{Log}\dot{\gamma}_1} \quad \text{Equation 2.7}$$

(Craig J, 2018).

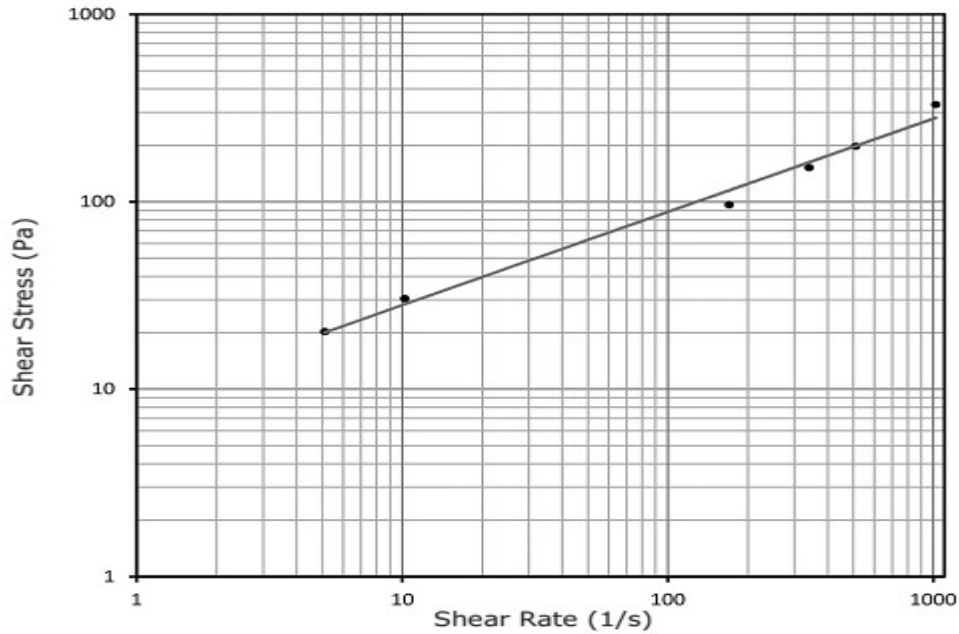


Figure 2.10 : Log-Log plot of Power law model (Bahrainian et al., 2018)

### 2.7.3 Herschel-bulkley model

The Herschel-bulkley model combines both the Bingham and Power law models and describes a pseudo-plastic fluid that requires yield stress to flow. It can be used to model fluid behaviour at both high and low shear rates and represents most drilling fluids more accurately than Bingham and Power law models. It is referred to as a three parameter model comprising of Plastic viscosity, yield stress and flow behavior. It is expressed mathematically as

$$\tau = \tau_H + K\dot{\gamma}^n \quad \text{for } \tau > \tau_H \quad \text{Equation 2.8}$$

Where  $k$  is consistency index and  $n$  is flow behaviour

$\tau_H$  is yield stress in pascal and  $\mathcal{T}$  is the magnitude of stress tensor

An initial calculation of yield stress must be made and shear stress minus yield stress versus shear rate can be plotted on a log-log scale (figure 2.10) to find fluid consistency  $k$  and flow behavior  $n$ . The yield stress for this three parameter model is calculated as

$$\tau_H = \frac{\tau_{max}^{\frac{2}{n}} - \tau_{min}^{\frac{2}{n}} \times \tau_{max}}{2\tau_{min}^{\frac{1}{n}} - \tau_{max}^{\frac{1}{n}}} \quad \text{Equation 2.9}$$

$\tau^c$  is the shear stress value which corresponds to geometric mean of shear rate  $\dot{\gamma}^*$  and is expressed as

$$\dot{\gamma}^* = \sqrt{\dot{\gamma}_{min}} \times \sqrt{\dot{\gamma}_{max}} \quad \text{Equation 2.10}$$

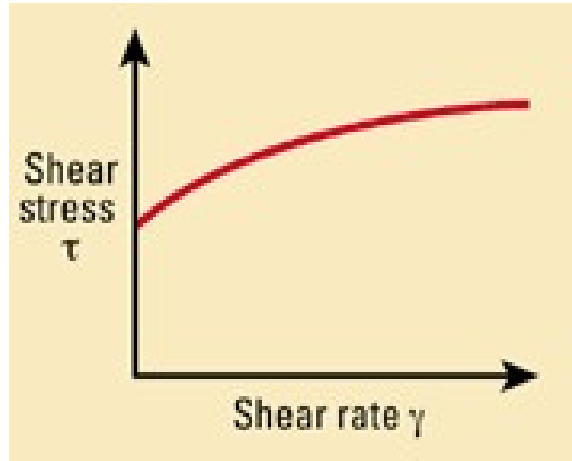


Figure 2.11: Herschel-Buckley fluid rheological behaviour (Slumberger Oilfield Glossary)

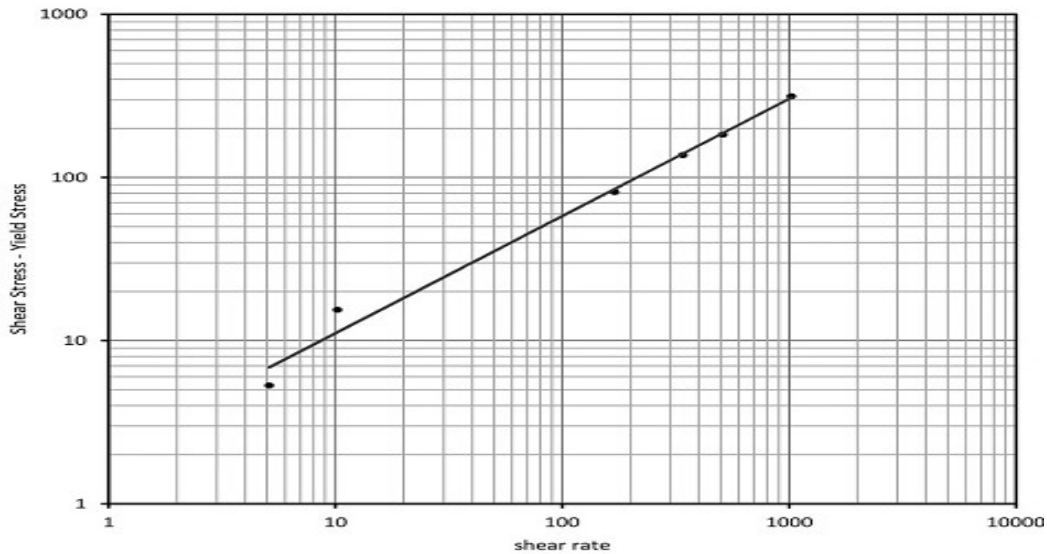


Figure 2.12 : Log-Log graph of Herschel-Bulkley model (Bahrainian et al., 2018)

#### 2.7.4 Casson model

Bahrainian et al., (2018) classified Casson model as a two parameter model used to predict oil suspension behavior. According to Hossain, (2016) Casson fluid requires two parameters to

characterize fluids. These parameters are yield stress,  $\tau_y$  and plastic viscosity,  $\mu_p$ . Above the yield stress, shear stress changes are linearly proportional to shear rate changes. Casson's model are useful in simulating fluids with plastic behavior like drilling fluids and give a higher accuracy than Bingham plastic model. The mathematical expression for Casson model is

$$\sqrt{\tau} = \sqrt{\tau_y} + \sqrt{\mu_p} \sqrt{\dot{\gamma}} \quad \text{Equation 2.11}$$

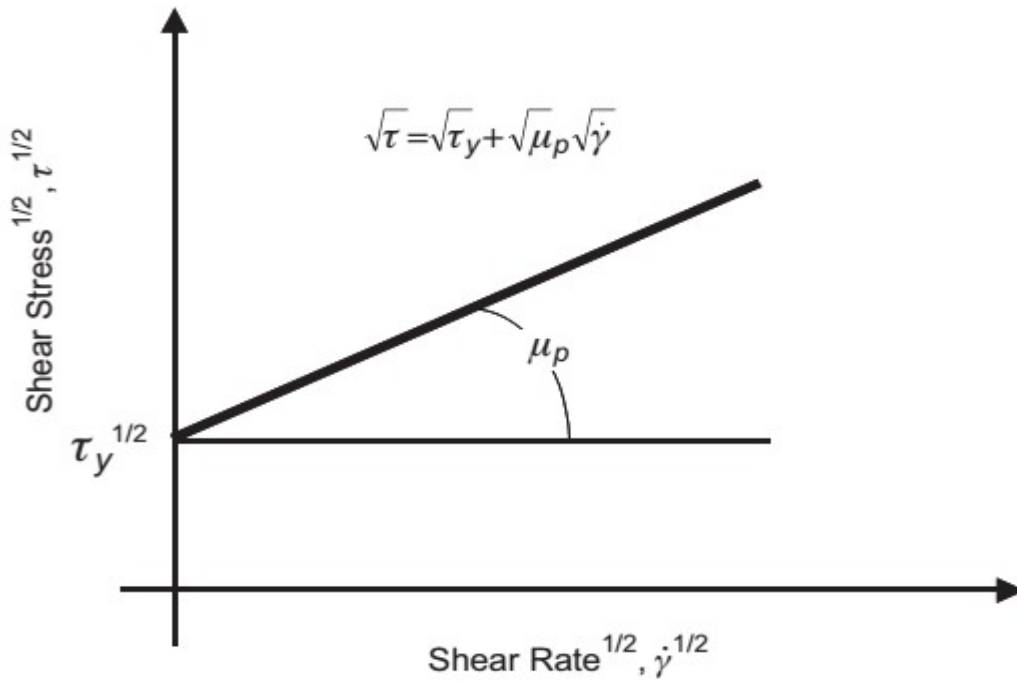


Figure 2.13: Graphical Representation of Casson model (Hossain, 2016)

### 2.7.5 Robertson-stiff model

Robertson-stiff model describes yield pseudo-plastic fluid slightly to be less accurate than Herschel Bulkley model (Hossain, 2016). It models drilling fluid and cement slurries (Bahrainian et al., 2018). It is expressed mathematically as

$$\tau = A(\dot{\gamma} + C)^B \quad \text{Equation 2.12}$$

A, B and C are constants in the model. The unit of constant A depends on B value. B is dimensionless and A has a unit of  $\text{dyne} \cdot \text{s}^B / \text{cm}^2$  or  $\text{g} / \text{cm} \cdot \text{s}^{2-B}$ . C is in  $\text{S}^{-1}$ . When  $C=0$ , Equation 2.12

describes a yield pseudo-plastic fluid and is Newtonian when  $B = 1$  and  $C = 0$ . Robertson stiff model has a similar graph representation with Herschel-bulkley model (Hossain, 2016).

### 2.7.6 Unified model

Unified model is an empirical model that derived its basis from Herschel bulkley model. It is used to describe the yield stress of pseudoplastic fluids (Zamora & Power, 2002). It has the same equation as that of Herschel-Bulkley but differs in its approach to estimate yield stress. The linearised Herschel-Bulkley equation as explained earlier and stated in Equation 2.13 is also required to get fluid consistency  $k$  and flow behaviour  $n$  (Håvard Stangeland, 2015).

$$\text{Log}(\tau - \tau_y) = \text{Log } k + n \text{Log } \dot{\gamma} \quad \text{Equation 2.13}$$

According to Zamora & Power, (2002), the yield stress can be gotten by taking  $\tau_y$  as low shear yield point expressed as  $\tau_{yL}$  and is given below.

$$\tau_{yL} = (2R_3 - R_6)1.066 \quad \text{Equation 2.14}$$

Where  $R_3$  and  $R_6$  are fann viscometer reading at 300 and 600 rpm in  $\text{lb}/100\text{ft}^2$

### 2.7.7 Api-model recommended practice 13 d model

A set of standards has been set by the American Petroleum Institute (API) for drilling fluid characterization known as API-RP 13D. This specification is recommended for bentonite-based mud with a wide range of shear rates (Clark, 2007). It comprises of drilling fluid property values and standards that are suitable for drilling purposes. It has been revised over the years. The recommended practice (RP) at providing a basic understanding of drilling fluid rheology and hydraulics and guidance to assist with drilling wells of various complexities, high-temperature/high-pressure (HTHP), extended-reach drilling (ERD), and highly directional wells.

Bingham plastic, power law, Herschel Bulkley and Casson models are the most commonly used rheological models to describe the behaviour of mud under stress conditions (Kazemi-Beydokhti & Hajiabadi, 2018).

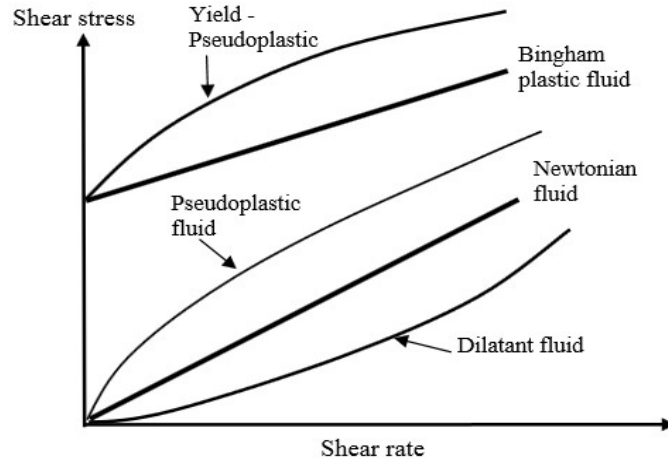


Figure 2-14: Newtonian and Non-Newtonian fluids (Nguyen & Nguye, 2012)

## 2.8 Hydraulics

Drilling hydraulics is an aspect of Drilling Engineering that deals with the flow and pressure associated with flow of fluid within the wellbore. The three primary functions of drilling fluids which are cutting transport, prevention of fluid influx, and maintenance of wellbore stability depends on the flow of drilling fluids and their associated pressure responsible for the flow (Hossain, 2016). Subsurface fluid pressure should be determined under three conditions namely:

- A static condition where well fluid and the central pipe are at rest.
- A circulating condition where fluid is pumped down the pipe and up the annulus between the central pipe and casing.
- Tripping in and out operation or when pipe is moved up and down. (Adam et al, 1986)

### 2.8.1 Pressure losses

Pressure losses are the most important parameter that should be determined accurately for proper selection of pump, drill bit, drill pipes, drilling rate, and other parameters to ensure good hydraulics (Saxena, Pathak, Ojha, & Sharma, 2017). Drilling fluid flowing down the drill strings and up the annulus must overcome frictional forces between the fluid layers, solid particles, pipe and borehole walls for efficient circulation. Hence, the pump pressure must overcome the combination of certain pressure losses. Mathematically, the pump pressure is a sum of the

pressure losses across surface equipment, drill pipes, drill collar, drill motor, drill bit, drill collar and drill pipe annulus and is expressed below

$$P_p = \Delta P_s + \Delta P_{dp} + \Delta P_{dc} + \Delta P_{mt} + \Delta P_b + \Delta P_{dca} + \Delta P_{dpa} \quad \text{Equation 2.15}$$

Where

$P_p$  = Pump pressure, psi or Kpa.

$\Delta P_s$  = Surface equipment pressure loss, psi or Kpa.

$\Delta P_{dp}$  = Drill pipe pressure losses, psi or Kpa.

$\Delta P_{dc}$  = Drill collar pressure losses, psi or Kpa.

$\Delta P_{mt}$  = Pressure drop inside mud motor, psi or Kpa.

$\Delta P_b$  = Drill bit pressure losses, psi or Kpa.

$\Delta P_{dca}$  = Drill collar pressure losses, psi or Kpa.

$\Delta P_{dpa}$  = Drill Pipe pressure losses. Psi or Kpa.

The total pressure losses excluding pressure losses at the bit is called parasitic pressure losses and is expressed as  $\Delta P_d$  given as

$$\Delta P_d = \Delta P_s + \Delta P_{dp} + \Delta P_{dc} + \Delta P_{dca} + \Delta P_{dpa} \quad \text{Equation 2.16}$$

In the absence of mud motor,

$$P_p = \Delta P_d + \Delta P_b \quad \text{Equation 2.17}$$

The drilling fluid system's pressure losses in the drill string and annuli can be determined by the following procedures

- The fluid average velocity should be determined at the point of interest either in the pipe or annulus.
- The average velocity is then used to get the Reynolds number and determine if the fluid is in laminar or turbulent flow regimes.
- The appropriate pressure loss equation pertaining to the flow regime and fluid rheology as stated in (Adam et al,1986) is used to calculate the pressure losses.

(Guo & Liu, 2011)

Pressure losses across the bit as expressed by (Adam et al,1986) is given as

$$\Delta P_b = \frac{\rho q^2 \times 8.311 \times 10^{-5}}{C_D^2 A_t^2} \quad \text{Equation 2.18}$$

Where

$\rho$  = Density of the mud, Ib/gal

q = Flow rate, gal/min

$C_d$  = Discharge coefficient

$A_t$  = Sum of the area of bit nozzles, Square Inches.

### 2.8.2 Cutting carrying capacity

The determination of lifting capacity of drilling fluid is complicated because the velocity of drilling mud increases from the walls and is maximum at the center of the annulus. The drill string rotates and exerts centrifugal forces on rock fragments which affect their location in the annulus. In practice, drilling personnel either increase the flow rate or effective viscosity when inefficient cuttings removal problems are encountered. However, this could also be dangerous as it reduces cleaning action and affects the rate of penetration of the bit (Adam et al,1986).

(Jr, Bruce, Oil, & Co, 1951) carried out some series of laboratory and field experiments to determine minimum annular velocity to remove cuttings and investigate the effect of drilling mud properties on cutting transport. It was observed that cuttings removal is improved with low viscosity and low gels, increased mud weights, turbulent flow in well's annulus, rotating action of the drill pipe, annular velocity being greater than particle slip velocity.

### 2.8.3 Hydraulic models

Several models have been created to predict hydraulics of drilling fluid in pipes. Sanghani, (1982) propounded a single-phase pseudoplastic fluid hydraulic pressure loss model. The model relates pressure losses to rheological parameters but did not take the pipe inclination angle and velocity regime (Laminar or Turbulent flow regime) into consideration. Pressure drop is expressed as

$$\frac{\Delta P_f}{\Delta L} = \frac{4K}{D} \left( \frac{8(3n+1)Q}{\pi n D^3} \right)^n \quad \text{Equation 2.19}$$

Where  $\frac{\Delta P_f}{\Delta L}$  is ratio change in frictional pressure drop to length of pipe in psi/ft , Q is flowrate of drilling fluid in gal/min and K and n are fluid consistency and flow behavior.

Pivnicka, Nguyen, Al-safran, & Saasen, (2015) predicted the pressure gradient of time-dependent drilling fluids in pipes under steady-state conditions by combining the momentum equation and rheological model parameters. The frictional pressure drop equation as a function of time at a given shear rate is as follows

$$-\frac{dp}{dL}(t, \dot{\gamma}) = \frac{4}{D} [\tau_1(\dot{\gamma}) e^{-\left(\frac{1}{T}(\dot{\gamma})t\right)} + \tau_{ye} + K \dot{\gamma}^m] \quad \text{Equation 2.20}$$

Where  $-\frac{dp}{dL}(t, \dot{\gamma})$  is frictional pressure loss as a function of time and given shear stress,  $\tau_{ye}$  , K and m are equilibrium yield stress ,fluid consistency and flow behavior. T is time constant and  $\tau_1$  is Pre exponential coefficient. Acceleration pressure drop component of the Total pressure drop in the pipe flow calculation as a function of fluid velocity with time is given as

$$\rho \frac{dv}{dt} = -\frac{dp}{dl_{accel}} \quad \text{Equation 2.21}$$

Where  $-\frac{dp}{dl_{accel}}$  is accelerational pressure drop ,  $\rho$  is the density in pounds per gal (lb/gal) and

$\frac{dv}{dt}$  is fluid velocity gradient with respect to time.

## Chapter 2

### **METHODOLOGY**

This chapter presents the materials, equipment and experimental design approach for the study.

#### **3.1 Materials/equipment**

##### **Clay sample collection**

Clay samples were collected by using hand auger to scoop the clay materials from dug pits at mining sites from Gombe state, Nigeria. The samples were collected from Balanga local government at location with latitude 6.97514° N and longitude 3.74545° E between Fila and Cham, Dongaje, Gombe state, Nigeria.

##### **Clay Purification and Processing**

The raw clay samples were purified to remove all gross impurities in the sample. Samples were ground using the electric grinder to reduce the particle size to less than 60 µm. The powder was wet sieved using distilled water to separate the clay from impurities such as rocks and sand. The resulting slurry was allowed to sediment and decanted. Wet sieved clay was air-dried to reduce the moisture content and thereafter oven-dried at 70 °C in an electric oven until a constant weight was achieved.

##### **Clay Beneficiation / Selection**

Clay beneficiation was carried out according to Akinwande et al (2014). The beneficiating agent that was employed was Na<sub>2</sub>CO<sub>3</sub> at concentrations ranging from 1.1 M to 5.5

M. The selection of the concentration range was based on a previous research by Salawudeen *et al.* (2014). The processed clay (100 g) was dispersed in 100 ml of distilled water to form slurry and the slurry was preheated to 60 °C for 5 minutes. The beneficiating agent (100 ml) was added to the preheated slurry and the mixture heated to 90 °C between 60 and 80 mins under continuous stirring. The slurry formed was sun-dried to reduce the moisture content and later oven-dried in an electric oven (Surgifield Laboratory oven, SM9053A) at 80 °C until a constant weight was achieved. The dried clay was ground to less than 100 microns using an electric grinder (Marlex Appliances PVT Limited).

The equipment used in this study to achieve the objectives are Zeiss Scanning electron microscope, Weighing balance, Sand Retort Kit, Multi-Mixer, Mud balance, variable speed rheometer in Materials Science and Engineering and Petroleum Engineering Laboratories of African university of Science and Technology, Galadimawa, Abuja.

**Scanning electron microscope (SEM):** The scanning electron microscope is an electron microscope that produces a surface image of samples with a focused beam of electrons is allowed to interact with the atoms of the samples thereby producing signals that display the surface topography and composition of the sample. Energy dispersed spectroscopy (EDS) involves the elemental analysis and chemical characterization of a sample through some source of X-ray excitation from a sample caused by allowing a focused beam of the electron into the sample



Figure 3.15: ZEISS SEM Equipment for SEM AND EDS Characterisation.

**Weighing balance:** Weighing scale or balance is a device used to measure the mass or weight of samples.



Figure 3.16: Weighing Balance

**Sand retort kit:** The volume of sand sized particles in the drilling fluid is determined by a sand content kit. Materials with size greater than  $74\ \mu\text{m}$  ( 200 mesh ) are sand particles and not fit for drilling usage.



Figure 3.17: Sand content kit.

**Multi-mixer:** To get accurate results from drilling fluid experiments, drilling mud samples in the process of their preparation are mixed thoroughly to create an homogeneous mixture. Multimixers are used to mix drilling mud samples in preparation for laboratory tests.



Figure 3.18: Ofite Multi-mixer

**Mud balance:** Mud balance is used to determine the density or weight of a given volume of liquid or drilling mud. It is are calibrated in pounds per gallon (lb/gal), specific gravity (SG, kg/m<sup>3</sup>), Pounds per cubic feet (lb/ft<sup>3</sup>),Pounds per square inch per 1000feet (lb/in<sup>2</sup>/1000ft).

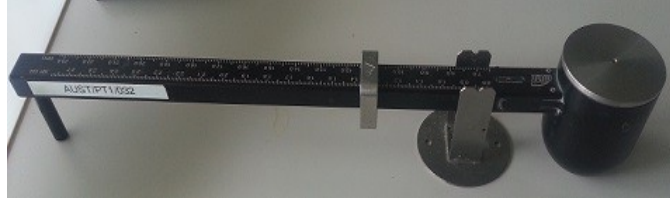


Figure 3.19: Ofite Mud Balance.

**Variable speed viscometer:** Variable speed viscometers are used to study rheological or flow behaviour of drilling mud suspensions. It gives the shear stress and shear rate relationship of drilling fluids with respect to time and temperature. Properties such as plastic and apparent viscosity, yield point, gel strength can be determined by the use of an 8 speed viscometer.



Figure 3.20: Ofite 8 speed viscometer model 800.

The materials used in the drilling mud formulations and their functions are given in the table below:

Component	Functions
Water	The continuous phase of the drilling mud sample
Modified Gombe Clay	Local based clay to be suspended in water
Barite	Weighting agent
Cassava Starch	Viscosifier and fluid loss additive
Corn Starch	Viscosifier and fluid loss additive
Gum Arabic	Viscosifier and fluid loss additive
Caustic soda(NaOH)	PH Modifier
Potassium Chloride(KCl)	Shale Inhibitor additive

Carbon Nanotubes	Fluid loss additive
------------------	---------------------

Table 3.1: Components of drilling mud formulations.

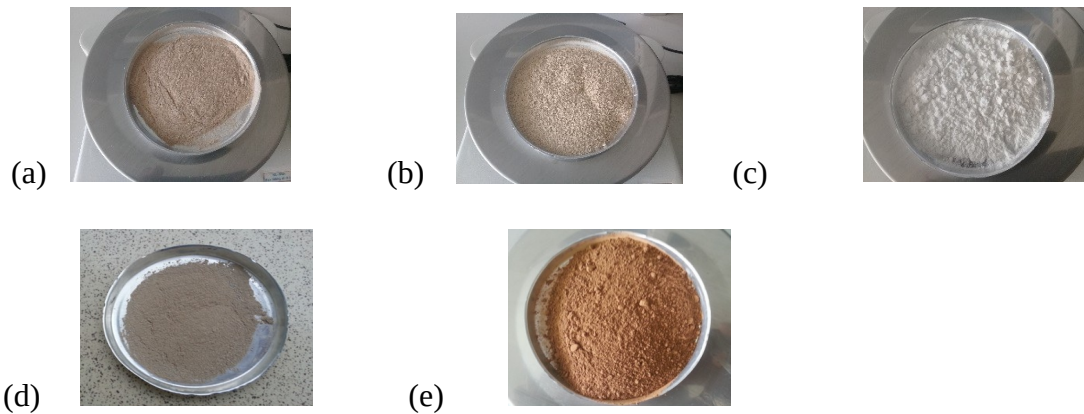


Figure 3.21:(a) Gum arabic sample (b) Corn Starch sample (c) Cassava Starch sample (d)Modified Gombe clay sample (e) Barite sample

### 3.2 Experimental design

The experimental design is in three stages and is shown below;

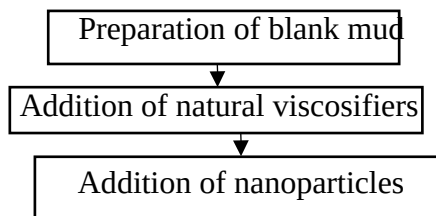


Figure 3.22: Experimental design

#### 3.2.1 Preparation of blank mud

- A water based mud is prepared with 24.5g of Gombe clay and 350ml of water. Density, Apparent and plastic viscosity, Yield point, Gel strength, solid content and thixotropy is taken immediately and after 24 hours to observe aging effect.
- The previous step is repeated with imported bentonite.

### 3.2.2 Addition of natural viscosifiers

- Three new mud formulations having 2g, 5g and 8g Corn starch in Hydrated Gombe clay mud samples is prepared and the density, apparent and plastic viscosity, Yield point, Gel strength, solid content and thixotropy is measured.
- The above procedure is repeated with Gum Arabic to give three formulations.
- Various new formulations are created using composite of gum arabic and cassava starch and their density, apparent and plastic viscosity, yield point, gel strength, solid content and thixotropy were measured.

### 3.2.3 Addition of nanoparticles

- The formulation in the previous stage with optimum property values close to API standard is selected
- Three new formulations by adding 0.1g,0.2g, 0.5g, 0.8g CNTs each to the previously selected mud formulation and thixotropic, filter and gel test is done at Room Temperature, 60°C and 94°F and the final mud formulation is selected.

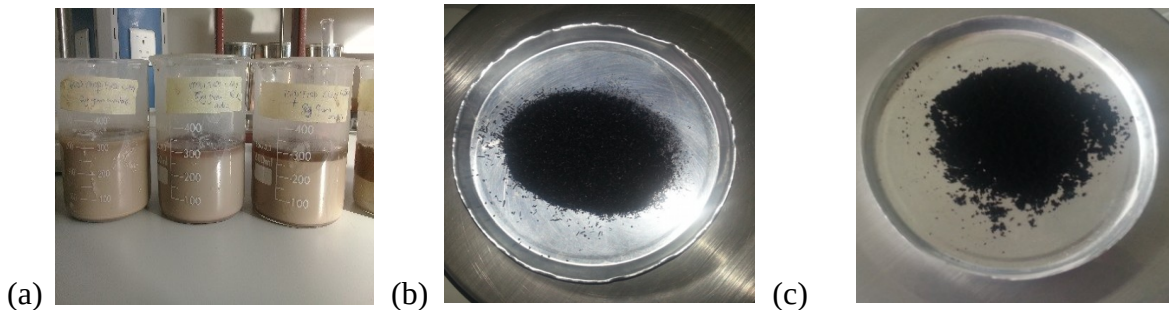


Figure 3.23(a): Modified Gombe based Mud Samples (b)Bamboo Raw but modified carbon nanoparticles (BRM) (c) Multiwall carbon nanotubes(MWCNT)

### 3.2.4 Rheology and hydraulics

Rheology of the finally selected Gombe mud is taken and the hydraulic pressure losses is determined using existing pressure loss models.

### **3.3 Procedures**

#### **3.3.1 Procedure for preparation of mud with and without additive**

A water base mud was prepared by dispersing 24.5g of Gombe clay in 350ml of water and stirred with a multi-mixer.

#### **3.3.2 Procedure to determine mud density**

- Mud mixture with or without additives was prepared and stirred with a multi-mixer and their temperature recorded.
- Then after, the mud balance base was placed on a flat level surface.
- The fill cup was filled with the mud sample. The lid was placed on the cup with care taken to prevent trapped air or gas. Some mud that expelled through the hole on the cap helped to ensure the cup is filled.
- The expelled mud was cleaned off the cup and arm and the balance placed on the knife edge. Afterwards, the rider was moved along the arm until the cup and arm was balanced. This is indicated by the bubble on the arm.
- Finally, the mud density was read at the edge of the rider towards the mud cup as soon as the bubble stabilizes.

#### **3.3.3 Procedure for solid content measurement**

- The sand content tube was filled to the indicated mark with drilling mud
- Afterward, the wash bottle was used to add water to the tube to raise its level to the next mark. While ensuring that the mouth of the tube was closed, the tube was shaken vigorously.
- Then after was the mixture poured onto a screen and water added to the tube to aid flushing of all mixtures onto the screen.
- The screen was flushed as well to make sure no sand particle is left on the mud remaining on the screen.
- The funnel was fitted upside down over the top of the screen. The assemble was inverted and the tip of the funnel placed on a mouth of a glass measuring tube
- Water is poured onto the screen to further flush sand left in the funnel.

- Finally, the tube containing the flushed sand and water mixture was allowed to settle to get a clear separation of the sand and water and the sand content is measured.

### 3.3.4 Procedure to determine rheology using 8-speed viscometer

- The test mud sample was placed in the sample cup and the rotor sleeve immersed in the mud to the fill line by raising the platform and tightening the locknut on the platform.
- Afterwards, the switch was pressed to turn on the device.
- The sample was mixed on the “STIR” setting for 10 seconds.
- Then after the knob was rotated to one of the speed settings and allowed to stabilize and the readings recorded. This is repeated for other speed settings and readings were taken from highest RPMs to lowest RPMs.

### 3.3.5 Procedure to determine gel strength using 8-speed viscometer

- The sample was mixed on “STIR” for 10 seconds
- Then after, the knob was rotated to “GEL” and the power was immediately shut off.
- As soon as the rotation of the sleeve stopped, the clock was set to 10 seconds after which the power was turned on and the maximum deflection was recorded as the dial reading which is the 10 seconds gel strength.
- To get the gel strength for 10 minutes, the sample was re-stirred for 10 seconds and the second and third step above was repeated by waiting for 10 minutes.

### 3.3.6 Calculations for rheology and API standards

According to Adam et al, 1986, apparent viscosity, plastic viscosity and yield point can be calculated with the expressions stated below.

$$\text{Plastic viscosity, } \mu_p = \Theta_{600} - \Theta_{300}$$

Equation 3.22

Where  $\Theta_{600}$  and  $\Theta_{300}$  is dial reading at 600 rpm and 300 rpm

$$\text{Apparent viscosity, } \mu_a = \frac{300\theta_N}{N}$$

Equation 3.23

Where  $\Theta_N$  is dial readings in degrees and N is the speed of rotor in revolution per minute.

*Yield point*  $T_y = \Theta_{300} - \mu_p$  *Equation 3.24*

Shear stress,  $\tau$  in pounds per 100 ft<sup>2</sup> (Ibf/100ft<sup>2</sup>) =  $\frac{Force}{Area} = \text{Dial reading} \times 1.067$

Shear rate, in per seconds (sec<sup>-1</sup>) = 1.701x Revolution per minute (RPM)

(Ofite manual, 2019).

The Table below gives API standards for drilling fluids properties

PROPERTIES	API STANDARD
Viscometer reading at 600RPM	minimum of 30cp
Density	8.65-9.5 Ib/gal
Plastic Viscosity	Less than 65 cp
Yield Point	15 to 45 Ib/100sq ft
Gel Strength at 10 seconds	3 to 20 Ib/100sq ft
Gel Strength at 10 Minutes	8 to 30 Ib/100sq ft
Filtrate Loss	15 ml max

Table 3.2: API standards for drilling fluid properties.

## CHAPTER 3

### PRESENTATION OF RESULTS AND DISCUSSION

In this chapter, materials characterization via SEM and EDS and thorough examination of experimental results and data analysis are presented and discussed.

#### 4.1 SEM and EDS characterisation of materials.

##### **SAMPLE X1: Modified Gombe Clay**

Modified Gombe clay is fine when viewed with the human eyes. SEM at 100 $\mu$ m shows its topography consists of roundlike particles of different sizes. It's elemental constituents are 42.4 wt% carbon, 3.9 wt% oxygen, 1.2 wt% sodium, 13.9 wt% aluminium, 28.41 wt% silicon, 0.35 wt% sulphur, 3.2 wt% potassium, 0.6 wt% tin and 6.15 wt% iron.

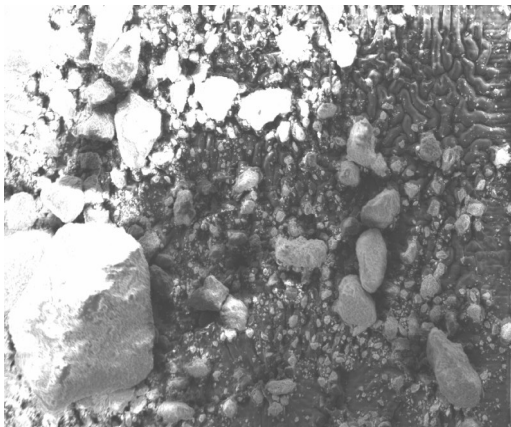
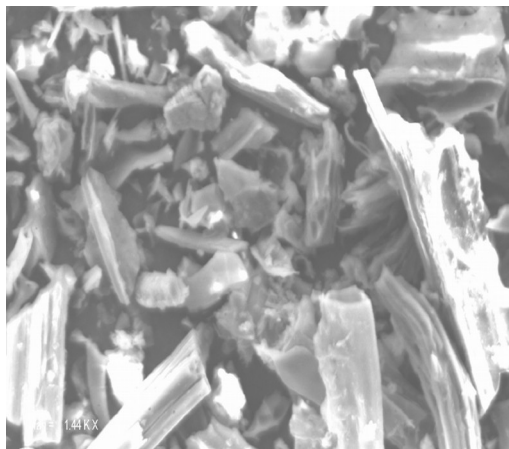


Figure 4.24: SEM Images of sample X1 at resolutions of 100  $\mu$ m

##### **SAMPLE X2: Modified raw bamboo**

Sample X2 is black and powdery when viewed with the human eyes. SEM analysis at 20 $\mu$ m and 10 $\mu$ m showed tube-like nature of particles as well their aggregation to each other. EDS showed that it comprised of mainly carbon (78.28% Carbon by weight) as well as minute portions of Silicon, Phosphorus, Potassium and Tin.



(a)

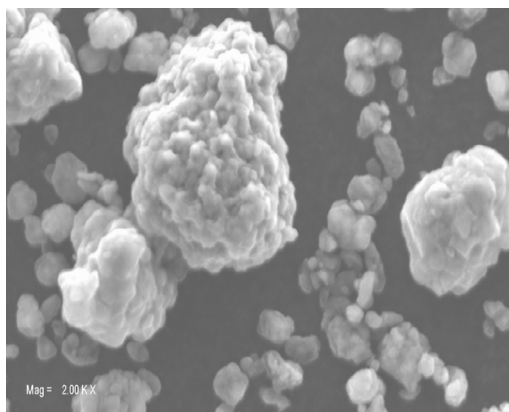


(b)

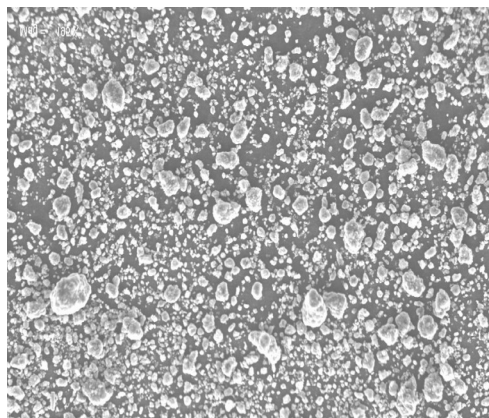
Figure 4.25: SEM images of sample X2 at resolutions of (a) 10  $\mu\text{m}$  (b) 20  $\mu\text{m}$

### **SAMPLE X3: Multiwall nanotubes**

Sample X3 is a dry black powder when observed with the naked eyes. SEM at 200  $\mu\text{m}$  and 20  $\mu\text{m}$  magnifications showed aggregated particles of different sizes with irregular rock-shaped geometry separated from each other and of different sizes. It comprises of carbon (100% carbon).



(a)



(b)

Figure 4.26: SEM Images of sample X3 at resolutions of (a) 20  $\mu\text{m}$  (b) 200  $\mu\text{m}$

**SAMPLE X4: Corn starch**

Corn starch at 100  $\mu\text{m}$  consist of clustered particle with no define shape. It has 35.03wt % Carbon, 25.11wt%, Nitrogen,21.58wt% Oxygen,0.37wt% Magnesium,2.12wt% Phosphorus, 3.49 wt% Molybdenum, 3.07 wt% Potassium and 9.23 wt% Calcium.

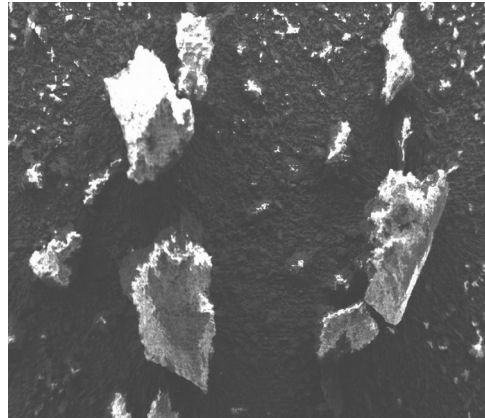


Figure 4.27: SEM Images of sample X4 at resolution of 100 $\mu\text{m}$

**SAMPLE X5: Cassava starch**

Cassava starch under SEM at 100  $\mu\text{m}$  displays tiny round like aggregated particles as seen in figure 4.5. It constituents in weight % are

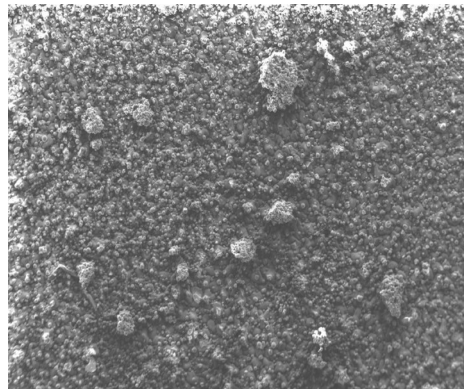


Figure 4-28: SEM Images of sample X5 at resolution of 100  $\mu\text{m}$

### **SAMPLE X6: Gum arabic**

Gum arabic samples was fine and powdery when viewed with the eyes. However, SEM at 100  $\mu\text{m}$  revealed that it comprised of irregular shaped solids of different sizes. Elemental compositions by wt% are 0.14wt% Carbon, 57.3wt% Oxygen, 2.5wt% silicon, 13.6wt% Potassium, 26.47wt% Calcium.

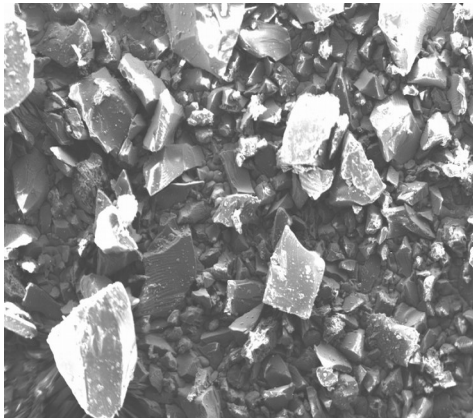


Figure 4.29: SEM Images of sample X5 at resolution of 100 $\mu\text{m}$

### **MINERAL COMPOSITION OF CLAY SAMPLES**

Untreated clay is composed of kaolinite -  $\text{Al}_2\text{Si}_2\text{O}_5(\text{OH})_4$ , quartz -  $\text{SiO}_2$  and low quality of montmorillonite -  $\text{Si}_{3.74}\text{Al}_{2.03}\text{Fe}_{0.03}\text{Mg}_{0.02}\text{O}_{11}$ . This result was similar to the one obtained by Apugo-Nwosu et al. (2011). The phase analysis of the treated clay sample clearly shows significant improvement in the quality of montmorillonite. The treated clay contains high quality montmorillonite -  $\text{Na}_{0.3}(\text{Al}, \text{Mg})_2\text{Si}_4\text{O}_{10} \cdot 8\text{H}_2\text{O}$ , Albite -  $\text{Na}(\text{AlSi}_3\text{O}_8)$ , kaolinite -  $\text{Al}_2\text{Si}_2\text{O}_5(\text{OH})_4$ , and  $\text{SiO}_2$  in form of Coesite.

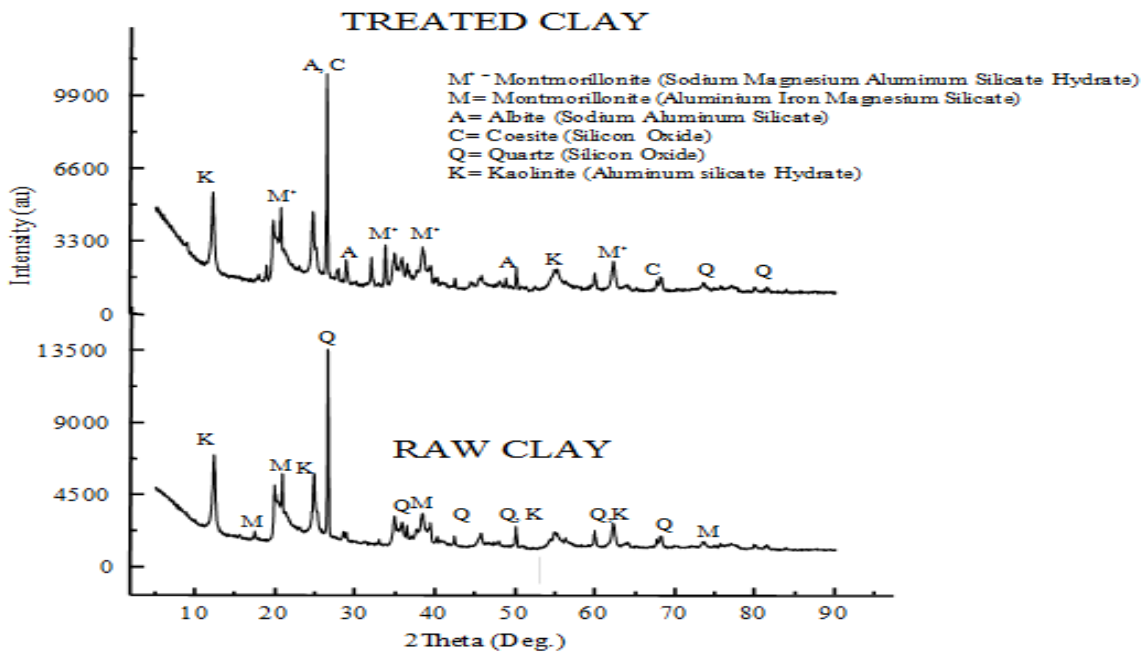


Figure 4-30: XRD showing Mineralogy of treated and untreated clay

#### 4.2 Rheology

Fifteen mud formulations with and without additives were prepared for sensitivity check on rheological properties to get the optimum or base formulation. 24 g of modified Gombe clay was dispersed in 350 ml of fresh water to give properties before and after aging for 24 hours obtained from experiments.

Table 4.3: Property values of mud formulations without additives

Properties	At start	After 24 hours
$\Theta_{600}$	3	3.5
$\Theta_{300}$	2	2
Plastic Viscosity	1	1.5
Apparent Viscosity	1.5	1.75
Yield Point	1	0.5
Gel strength at 10 seconds	1	1
Gel strength at 10 minutes	1	1
Density, lb/gal	8.7	8.7
Temperature, °C	27	24
Sand content	< 1%	< 1%

Table 4.1 above shows little or no difference in the properties of the mud after 24 hours of aging. Rheological properties and sand content of the blank mud formulation before and after aging were quite low with no potential threat to drilling operations according to API requirements. However, the mud formulated still needs some improvements. To enhance the rheological properties, new muds formulations laden with Corn Starch, Gum Arabic, and Cassava Starch additives were prepared and their properties were tested at room temperature. In Table 4-2, it is observed that as the mass of corn starch increased from 2 to 15 g the plastic viscosity increased accordingly. However, Yield point and gel strength at 2 and 5 g remained almost constant but increased a little upon addition of 8 and 15 g concentrations. As the concentrations of Gum arabic increased between 2 to 20 g, Plastic and Apparent viscosities increased accordingly. Gel strength was observed to decrease with the addition of 2, 5 and 15g concentration, the gel increased to its previous value as before and at 20 g, it increased a little at 10 minutes gel. These properties of the mud formulations with additive proved to have changed on the addition of various additives but not yet up to the optimum standard required for drilling purposes. This suggests that new formulations that meet optimum requirements are required. It is observed that the mud sample was more responsive and suited to Gum arabic compared to Corn starch. Since

the values already obtained are not sufficient enough, composites of additives in muds were prepared. The mud formulation with 20 g gum Arabic and 20 g cassava starch showed tremendous improvement on plastic and apparent viscosities and yield point. However, the gel strength values remained poor.

Table 4.4: Mud Formulations with additives

<b>Drilling mud Formulations</b>	<b><math>\Theta_{600}</math></b>	<b>PV</b>	<b>YP</b>	<b>10'</b>	<b>10''</b>	<b>Density (lb/gal)</b>	<b>Temperature, °C</b>
Hydrated mud + 2g corn starch	4	1.5	1	1	1	8.5	30
Hydrated mud + 5 g corn starch	6	2.5	1	1	1	8.75	30
Hydrated mud + 8g corn starch	8	4.5	-1	1	1.5	8.8	29.4
Hydrated mud + 15 g corn starch	9.5	5.5	-1.5	1.5	3	8.82	29
Hydrated mud + 2g gum arabic	4	1.9	0.2	0.5	0.5	8.65	29.5
Hydrated mud + 5g gum arabic	5	2.5	0	1	1	8.7	29.7
Hydrated mud + 8g gum arabic	7	3.5	0	1	1	8.79	30.5
Hydrated mud + 10g gum arabic	10	4.5	1	1	1	8.91	30.2
Hydrated mud + 15g gum arabic	18.5	10.5	-2.5	1	1	8.95	28.5
Hydrated mud + 20g gum arabic	29.5	18.5	-7.5	1	2.5	8.98	28.2
Hydrated mud + 15g cassava starch	4	1.9	0.2	1	1	8.8	29.5

Hydrated mud + 10g cassava starch +15g gum arabic	25	13	-1	1	1	8.93	26
Hydrated mud + 20g cassava starch +20g gum arabic	41.5	22.5	-3.5	1	1	9	30.5

PV =Plastic Viscosity, YP= Yield Point, 10’= 10 seconds gel strength .10”= minutes gel strength,  $\Theta_{600}$  =Dial Reading at 600RPM.

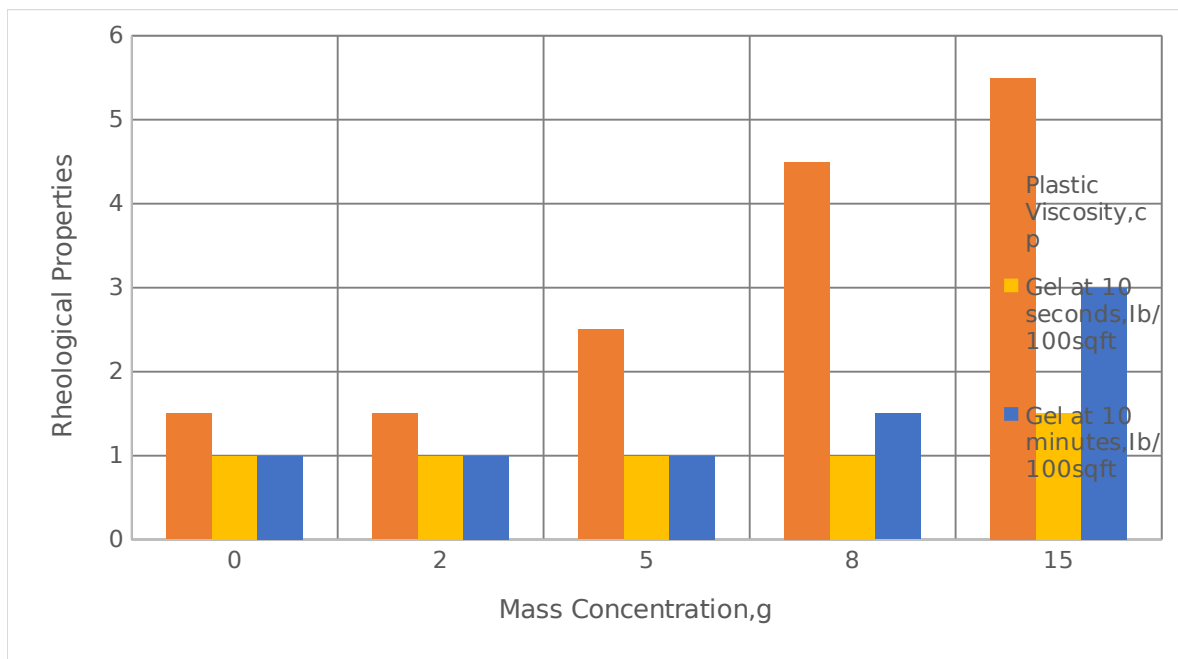


Figure 4.31: Chart showing rheological properties of mud before and after addition of corn starch at various concentration

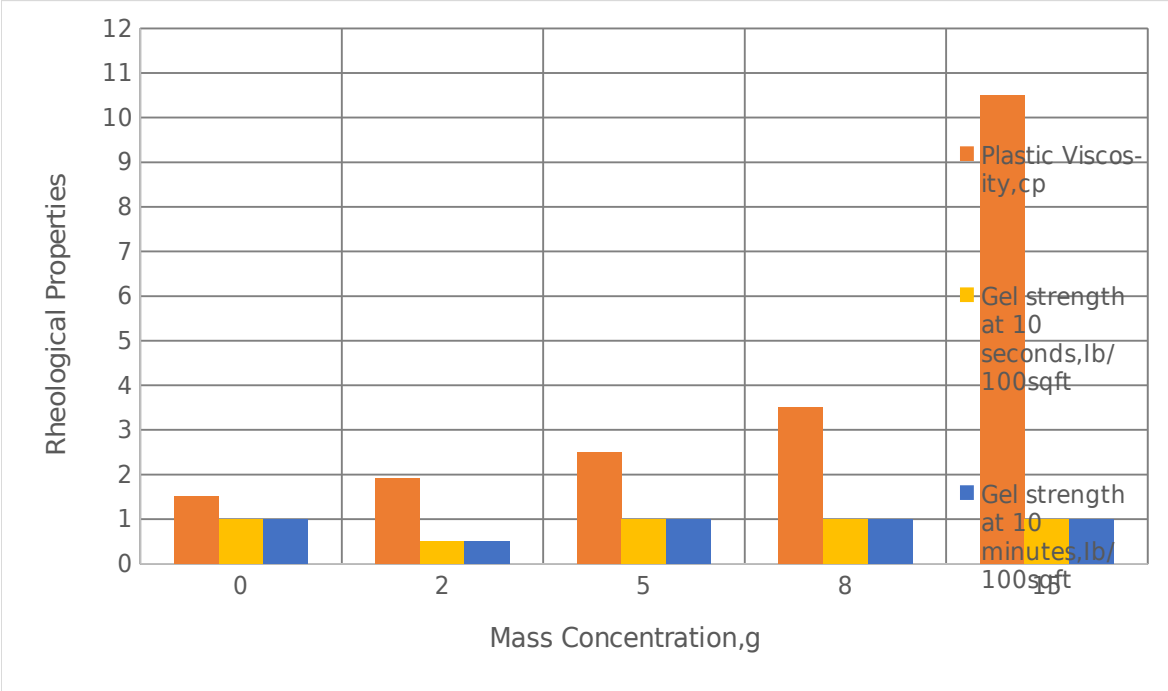


Figure 4.32: Chart showing rheological properties of muds before and after addition of gum arabic of various concentration.

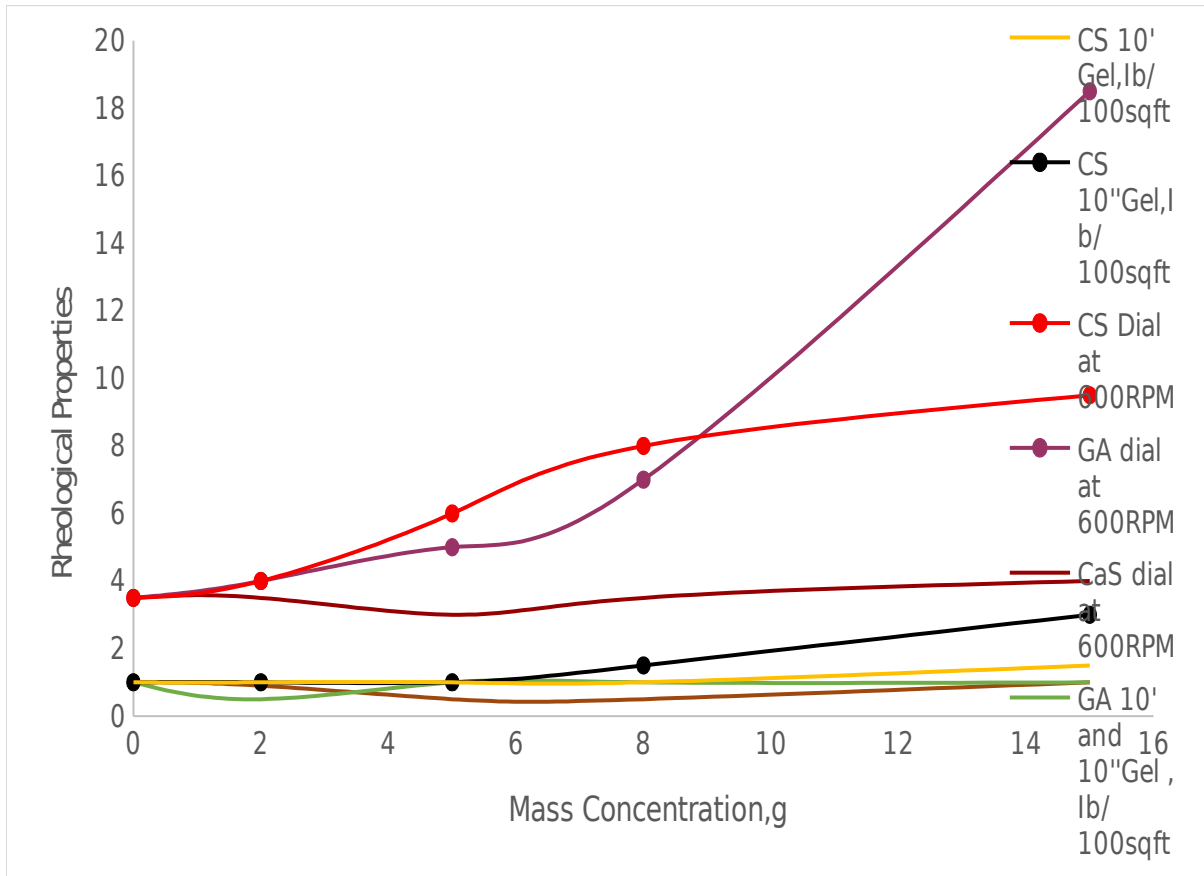


Figure 4.33: Comparison between Cassava starch, Gum Arabic and Corn starch 600rpm and gel behavior in mud

From Table 4.2, the formulation of hydrated mud with 20g cassava starch and 20g gum Arabic was selected for further beneficiation considering the closeness of its dial reading at 600 rpm, plastic and apparent viscosities to API standards compared to other formulations. NaOH and KCl were added to increase the pH and salinity for shale inhibition of the mud. Barite was added as well as a weighting agent. Table 4-3 shows the weighted and non-weighted mud formulations.

Table 4.5: Weighted and Unweighted mud formulations at room temperature.

MATERIALS	WEIGHTED MUD FORMULATION	UNWEIGHTED MUD
-----------	--------------------------	----------------

		FORMULATION
Fresh water (ml)	350	350
Gum Arabic (g)	20	20
Cassava Starch (g)	20	20
KCl (g)	20	0
NaOH (g)	0.25	0
Barite (g)	75.4	0

Rheological properties of the weighted and unweighted mud formulations in Table 4.3 are shown in Table 4.4 .The rheology of the weighted 20 g cassava starch and 20 g gum Arabic formulation compared to the unweighted 20 g cassava and 20 g gum arabic is presented in figure

Table 4.6: Rheological properties of weighted and unweighted mud formulations at room temperature in comparison to API standard.

Rheological Properties	Weighted mud formulation	Unweighted mud formulation	API Standard
Dial Reading at 600RPM	47	41.5	Minimum 30
Plastic viscosity, cp	23	22.5	Less than 65cp
Yield Strength, Ib/100sqft	1	0	15 to 45
Gel Strength at 10 seconds, Ib/100sqft	1.5	1	3 to 20
Gel Strength at 10 minutes, Ib/100sqft	2	1	8 to 30

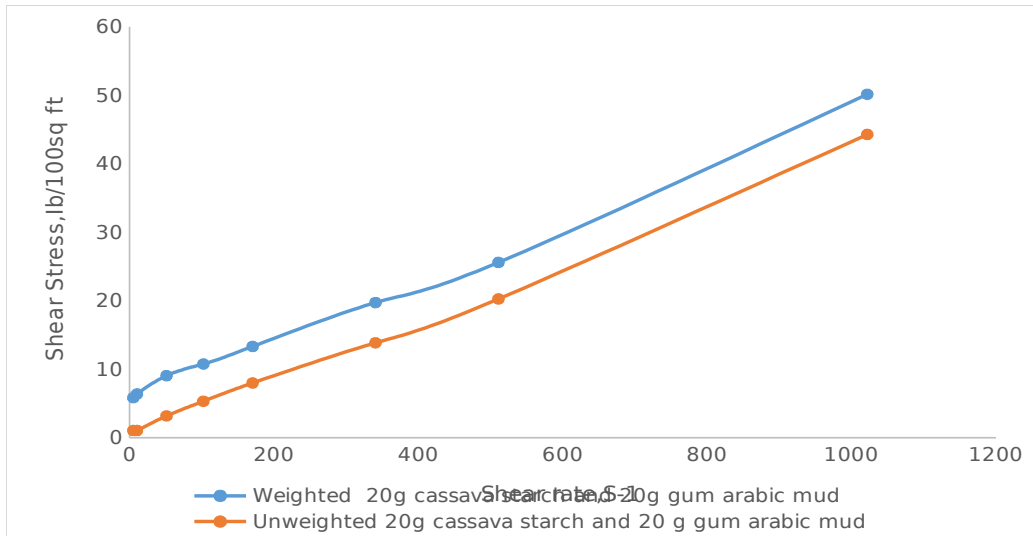


Figure 4.34: Comparison between rheology of weighted and unweighted 20g cassava starch and 20g gum arabic mud formulations.

Figure 4.11 shows the shear stress-shear rate relationship between weighted and unweighted 20g cassava starch and 20g gum arabic mud formulations. It is observed that at similar shear rate both formulation exhibited different shear stresses. The weighted 20g cassava starch and 20g gum arabic required greater shear stress compared to the unweighted 20g cassava starch and 20g gum arabic formulation. This signifies an increase in yield stress and gel strength for the weighted formulation compared to the unweighted one. In the bid to improve rheological properties to API standard, the weighted formulation was chosen and further benefited using nanoparticles (Multiwall nanoparticles and Bamboo raw and modified).

Tables 4.5 below contains types, materials and their concentration used in formulation of different weighted muds and the properties of the mud formulations.

Table 4.7: Types and concentrations of materials used in the formulated weighted drilling muds.

Mud sample	Material used in the preparation of mud	Material concentration (g)
Base weighted Mud	Bentonite	24.5ml
	Gum Arabic, GA	20g
	Barite	75.4g
	NaOH , CS	0.25
	KCl	20g

MWCNT Mud	Bentonite	24.5ml
	Gum Arabic, GA	20g
	Barite	75.4g
	NaOH , CS	0.25
	KCl	20g
	MWCNT	0.1 – 0.8
BRM Mud	Bentonite	24.5ml
	Gum Arabic,GA	20g
	Barite	75.4g
	NaOH , CS	0.25
	KCl	20g
	BRM	0.1 – 0.8

#### 4.2.1 Effect of temperature on rheology of base weighted mud formulation

The base weighted mud formulation was subjected to a temperature of 25, 60 and 94 °C. Figures 4.10, 4.11 and 4.12 shows the effect of temperature on plastic viscosity, yield point, and gel strength. Plastic viscosity and yield point are reduced with an increase in temperature. Plastic viscosity decreased as the weighted mud sample temperature increased from 25 to 60 °C. This behavior is probably because some of the particles in the mud sample have been destroyed due to thermal effects. However, at 94 °C, plastic viscosity being very high could be the result of the evaporation effect leaving a larger ratio of the concentration of solids to liquids. Hence, the solid particles attracted each other more closely. Gel strength at 10 seconds and 10 minutes increased as temperature increased from 25 to 94°C. The yield point and gel strength are measures of attractive forces between particles in the mud. An increase in temperature of the mud from 25 to 94 °C increased to yield point and gel strength. This is probably due to the evaporation effect that has occurred during the heating process from 25°C to 94 °C causing an increase in the ratio of attracted solid particles to the liquids.

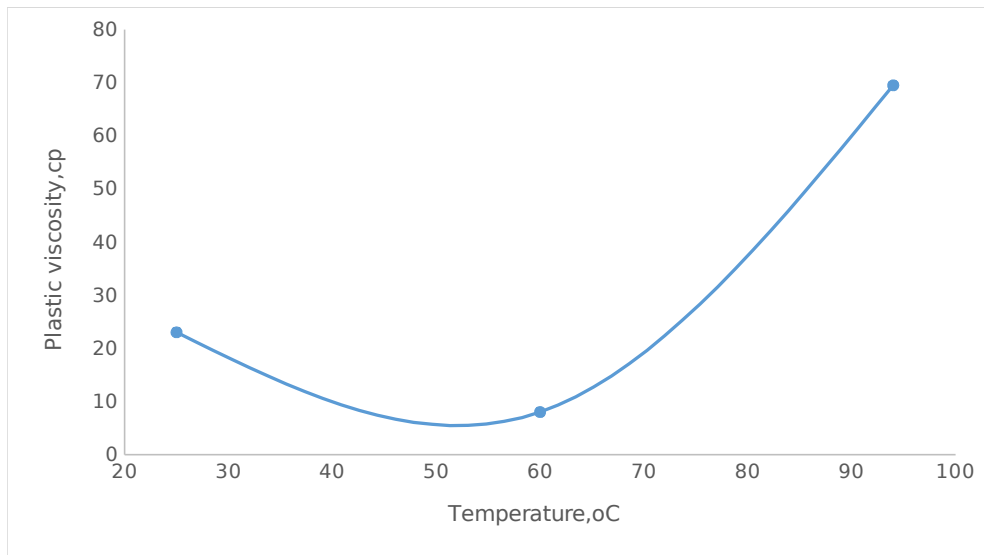


Figure 4.35: Plastic viscosity against temperature for base weighted mud formulation

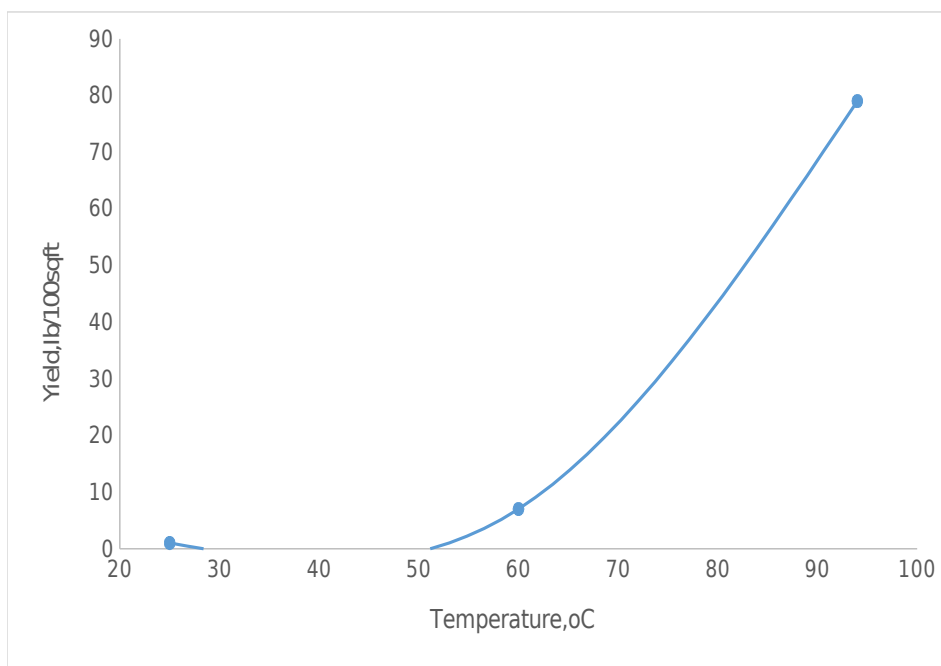


Figure 4.36: Yield Point versus Temperature for base weighted mud formulation

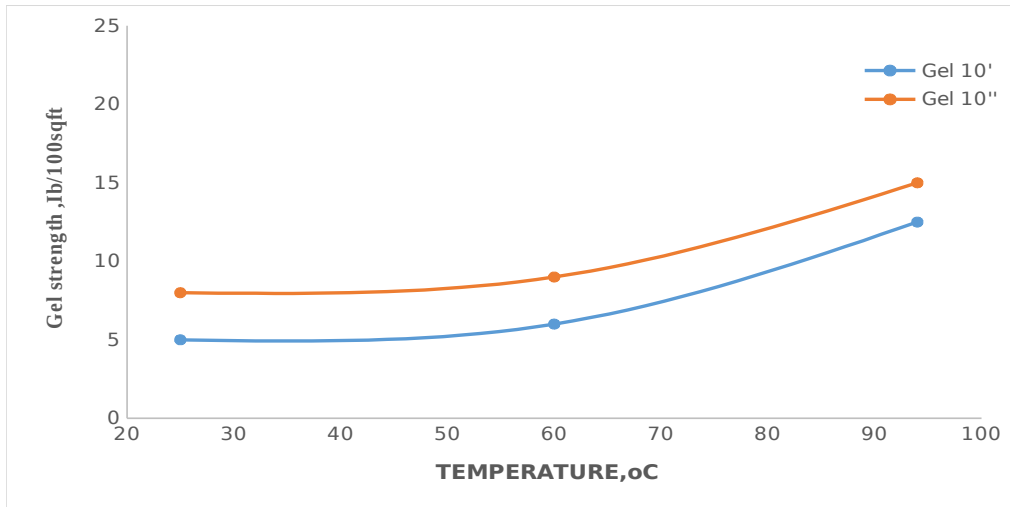


Figure 4.37: Gel strength versus temperature for base weighted mud formulation

#### 4.2.2 Effect of nanoparticles on rheology of base weighted mud formulations.

Nanoparticles applications in drilling fluid have helped to improve the rheological of the fluid. 0.1, 0.2, 0.5 and 0.8 g Multiwall CNTs and activated bamboo carbon (BRM) were added to the various base weighted mud samples to investigate their effect on the rheological properties of the mud sample at temperatures of 25, 60 and 94 °C. Table 4.6 and 4.7 shows their effect on the weighted drilling mud formulations.

Table 4.8: Effects of MWCNT on drilling mud

MWCNT Conc. g	Temperature (°C)	Dial Reading@600RPM	Dial Reading@300 RPM	PV, cp	Yp	Ge l 10'	Ge l 10''
0	26	47	24	23	1	5	8
	60	23	15	8	7	6	9
	94	218	148.5	69.5	79	12.5	15
0.1	26	39.5	18.5	21	-2.5	5	9
	60	21.5	13	8.5	4.5	5	7
	94	218	145	73	72	30.5	29.5
0.2	26	39	18	21	-3	5	8
	60	20.5	12.5	8	4.5	5	7

	94	207	155	52	103	25	24
0.5	26	37	20	17	3	5	8
	60	24	14.9	9.1	5.8	5	8
	94	240	188.5	51.5	137	24	21
0.8	26	36.2	19	17.2	1.8	5	7.5
	60	24	14	10	4	5	8.5
	94	251.5	177	74.5	102.5	22.5	19.5

Table 4.9: Effects of BRM on drilling mud

BRM conc. g	Temperature (°C)	Dial Reading@600 RPM	Dial Reading@300 RPM	PV, cp	Yp	Gel 10'	Gel 10"
0	26	47	24	23	1	5	8
	60	23	15	8	7	6	9
	94	218	148.5	69.5	79	12.5	15
0.1	26	43.5	18	25.5	-7.5	5.5	8.5
	60	24	14.5	9.5	5	5.5	7.5
	94	224	142	82	60	26.5	25
0.2	26	40.5	17.5	23	-5.5	5	6
	60	25.5	15.5	10	5.5	4	5
	94	207	142.5	64.5	78	18	17
0.5	26	40	21	19	2	4.5	7
	60	21	13	8	5	5	8
	94	220	147	73	74	17.5	16.5
0.8	26	39.5	18	21.5	-3.5	4.5	6.5
	60	23	13.5	9.5	4	5	8.5
	94	224	145	79	66	17	15

### Sensitivity of different concentration of MWCNT and BRM on gel.

Figure 4.13 to 4.14 shows the effect of MWCNT and BRM on gel at 26.64, 60 and 94 °C. The figures show that at 26.64 °C there is little or no changes in gel strength at 10 seconds and 10 minutes. Gel strength at 10 seconds and 10 minutes was improved by the addition of nanoparticles at all concentrations at 94 °C. However, the increase was most significant between 0.1 and 0.2 g of MWCNT and BRM. Afterward, there is a decline in gel strength as the concentration increases to 0.8 g. MWCNTs formulations produced gel greater than BRM formulations mostly. It is observed at 94 °C that the CNTs act as thinner causing a reduction in plastic viscosity and gel strength in the mud as it's concentration increases beyond 0.2g. This means that CNTs concentrations beyond 0.2g would be too excessive and reduce cutting suspension ability at 94 °C. An estimate of 0.1g MWCNT formulation is selected for further analysis.

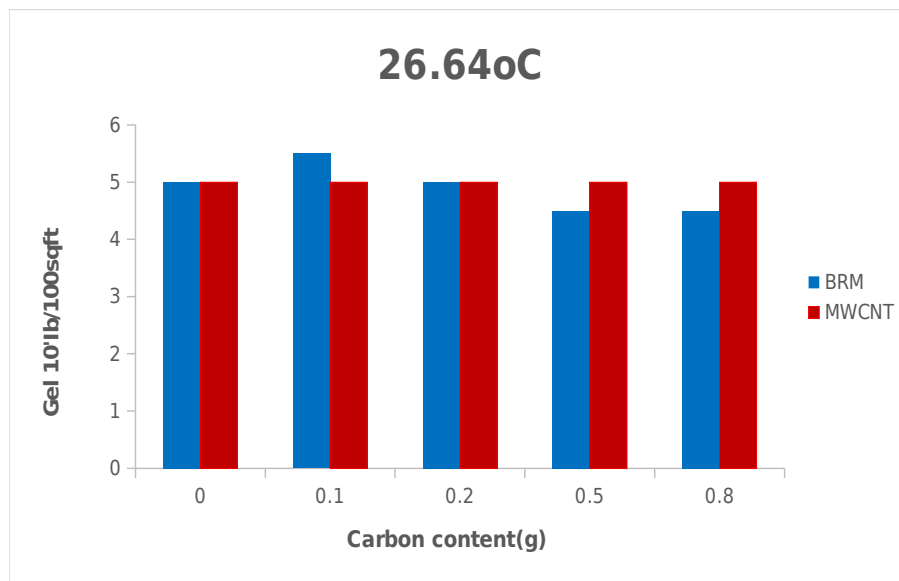


Figure 4.38: Effect of MWCNT and BRM on 10 seconds gel at 26.64°C

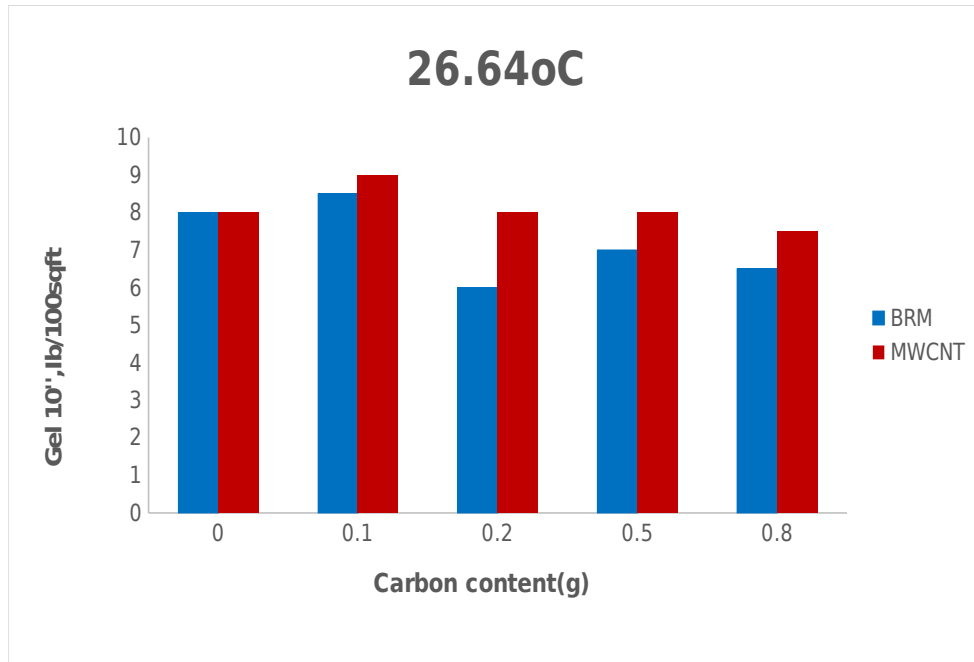


Figure 4.39: Effect of MWCNT and BRM on 10 minutes gel at 26.64°C

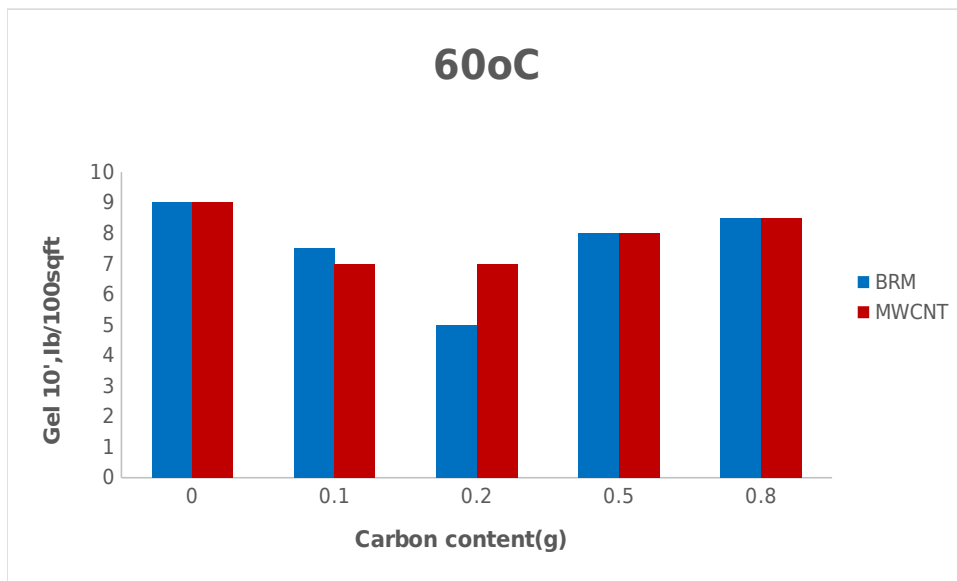


Figure 4.40: Effect of MWCNT and BRM on 10 seconds gel at 60°C

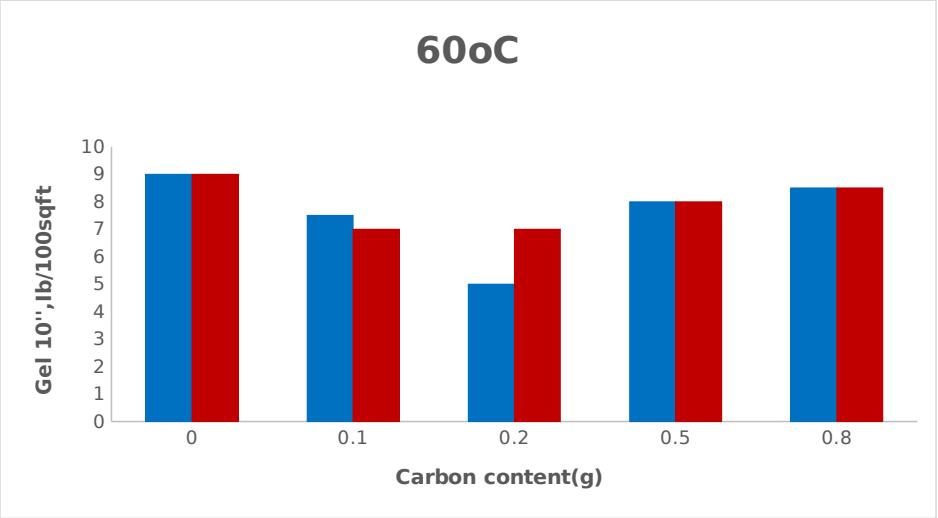


Figure 4.41: Effect of MWCNT and BRM on 10 minutes gel at 60°C

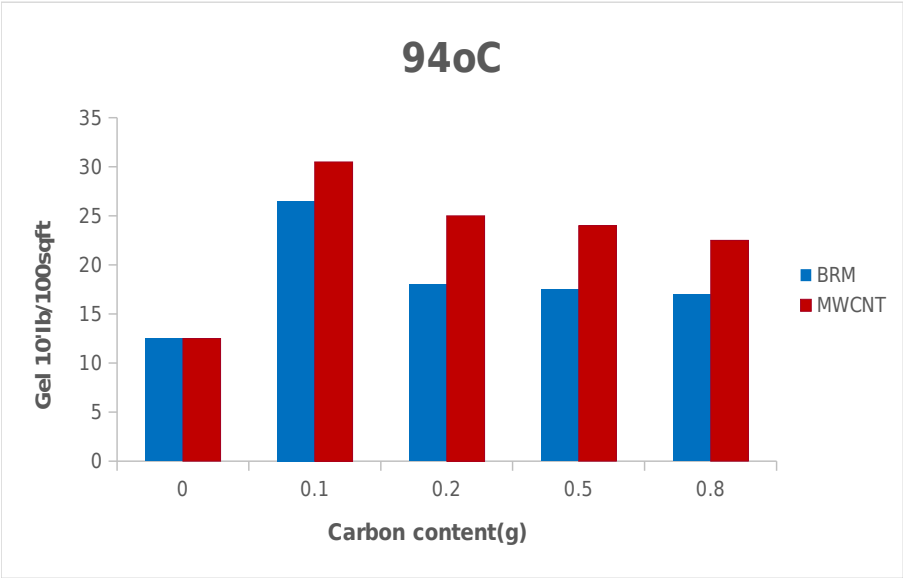


Figure 4.42: Effect of MWCNT and BRM on 10 seconds gel at 94°C

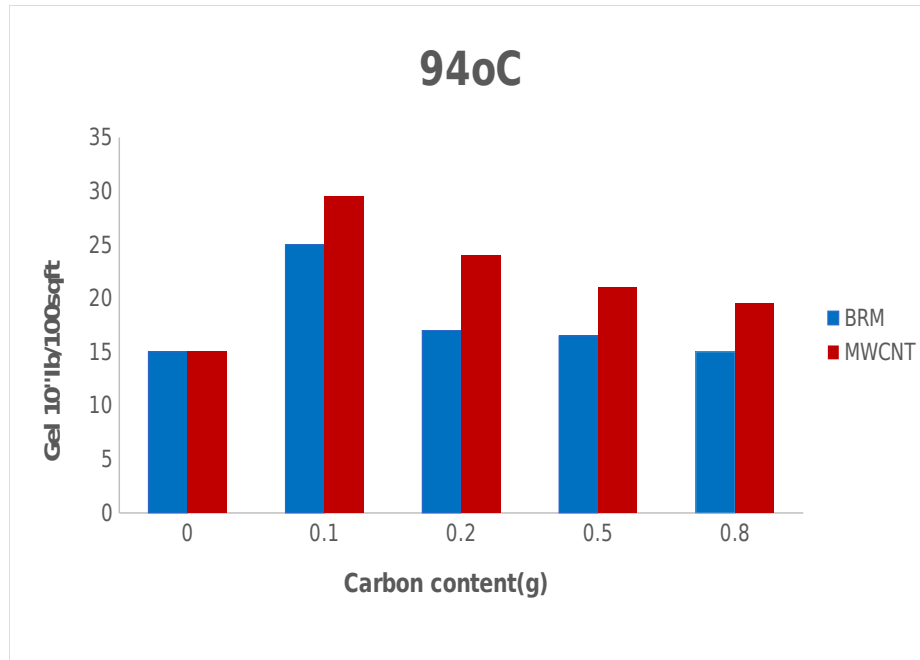


Figure 4.43: Effect of MWCNT and BRM on 10 minutes gel at 94°C

#### Effect of MWCNT and BRM on gel strength at different temperatures

Figure 4.19 and 4.20 shows the effect of MWCNT and BRM on gel strength at different temperature. The plot shows that an increase in temperature at various concentrations of MWCNT and BRM resulted in an increase in gel strength. This shows that particles tend to be more aggregated as temperature increases in the presence of MWCNT and BRM. MWCNT and BRM mud helped to increase gel strength.

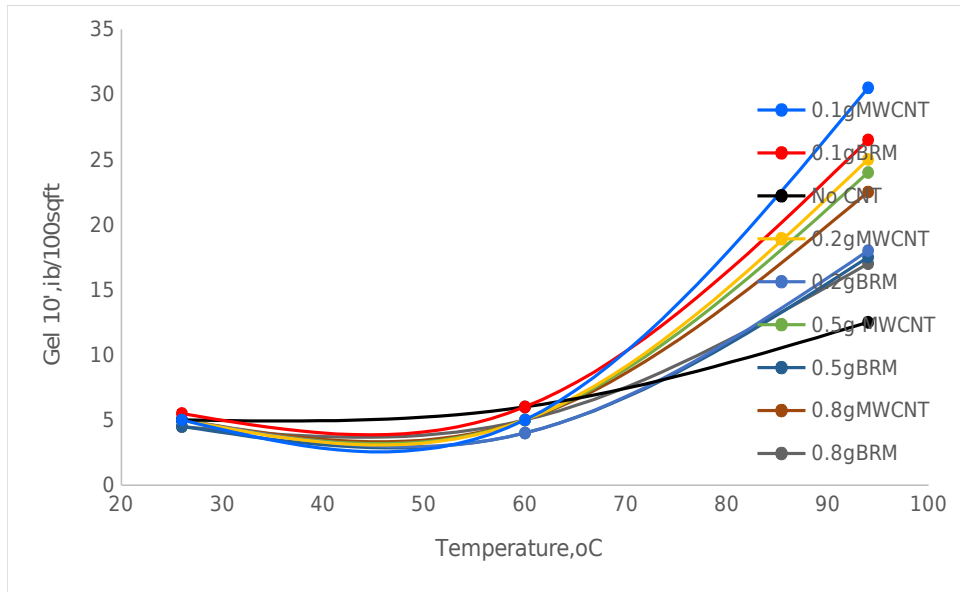


Figure 4.44: Effect of 0.1g, 0.2g, 0.5g and 0.8g concentrations of MWCNT and BRM on 10 seconds gel at different temperatures

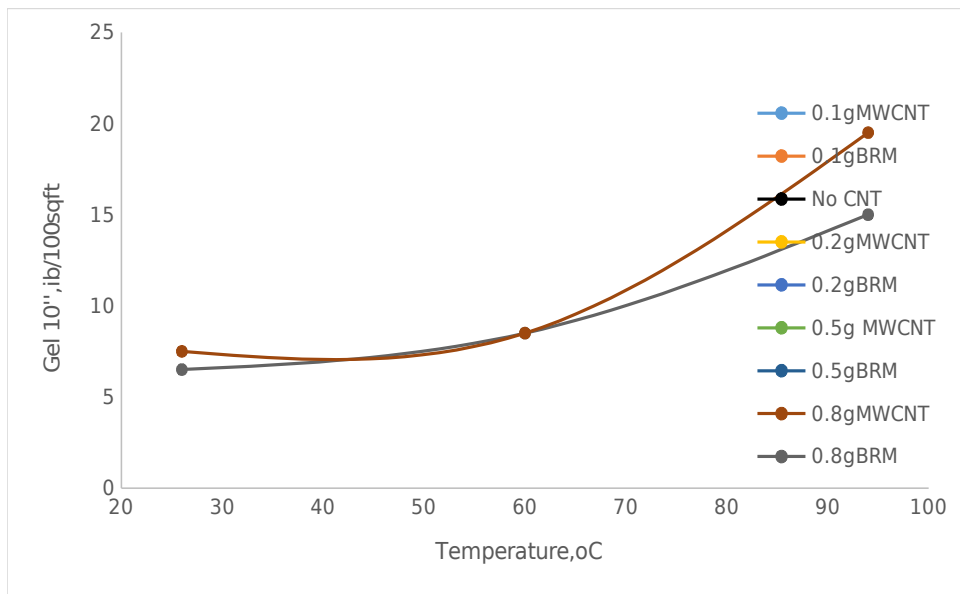


Figure 4.45: Effect of 0.1g, 0.2g, 0.5g and 0.8g concentrations of MWCNT and BRM on 10 minutes gel at different temperatures

### Effect of MWCNT and BRM on plastic viscosity at different temperatures

Plastic viscosity is a measure of the resistance to flow as a result of the solid particles present in the mud. Plastic viscosity in the presence of MWCNT and BRM declined from room temperature to 60 °C and then followed a rapid increase at 94 °C. The decline could be the result of partial destruction of some particles due to heating. However, the evaporation effect was more dominant at 94°C leaving a high solid content and hence, higher plastic viscosity values. Some values of plastic viscosity of MWCNT and BRM muds were higher or less compared to formulation with no CNT.

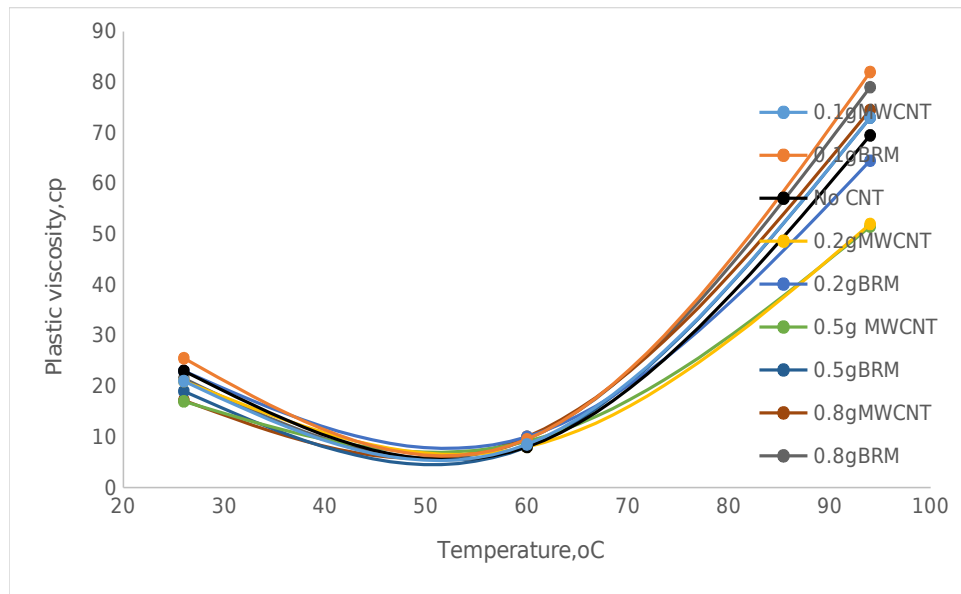


Figure 4.46: Effect of 0.1g, 0.2g, 0.5g and 0.8g concentrations of MWCNT and BRM on Plastic viscosity at different temperatures

### Effect of MWCNT and BRM on yield point at different temperature

The yield point and gel strength have similar properties because they are both affected by particle aggregation and hence, figure 4.22 shows a similar trend in comparison with figures 4.19 and 4.20. The plot shows that as temperature increases, the yield point also increases. When compared to the formulation without CNTs, some MWCNT and BRM formulations gave higher values of yield point.

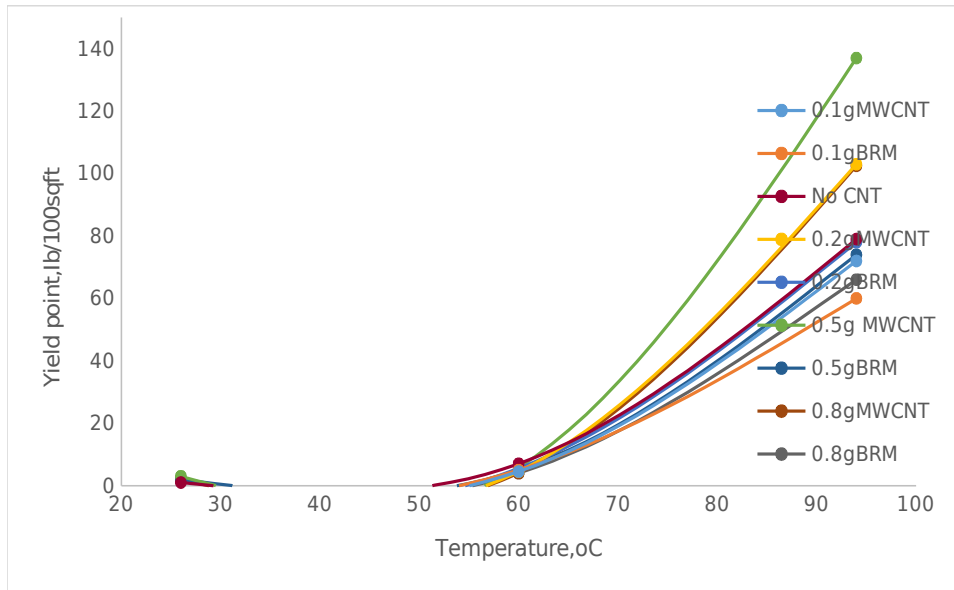


Figure 4.47: Effect of 0.1g, 0.2g, 0.5g and 0.8g concentrations of MWCNT and BRM on yield point at different temperatures.

### 4.3 Rheological models and consistency plots

From all the tables and figures of MWCNT and BRW weighted mud formulations effect, it is observed that optimum values of the drilling mud lies between the 0.1g and 0.2g MWCNT formulations and also between 0.1g and 0.2g BRM formulations. In this section, models of an estimate of the optimum which is at 0.1g MWCNT at room temperature and 94°C is created using Bingham, Power-law and Herschel-Bulkley models using regression. This is shown below from Figures 4.28 to 4.39. Consistency plots are shown below to compare the effect of 0.1g MWCNT and BRM on Base weighted mud formulations. It is observed that at room temperature the Base weighted mud formulation exhibited greater shear stress at both low and high shear rates compared to the 0.1g MWCNT and 0.1g BRM formulations indicating higher values for apparent viscosity, yield point and gel strength compared to CNT formulations. At 60°C apparent viscosity, yield point and gel strength values for 0.1g BRM formulation were highest at low shear rates compared to the Base weighted mud formulation and 0.1g MWCNT formulation. However, at 94°C, 0.1g MWCNT formulation had greater shear stress values at both low and high shear rates compared to the Base weighted mud formulation and 0.1g BRM formulations indicating

higher values for apparent viscosity, yield point and gel strength compared to Base and 0.1g BRM formulations.

**Consistency plot for 0.1gMWCNT and 0.1gBRM**



Figure 4.48: Consistency plot for 0.1g MWCNT and 0.1g BRM at 26°C

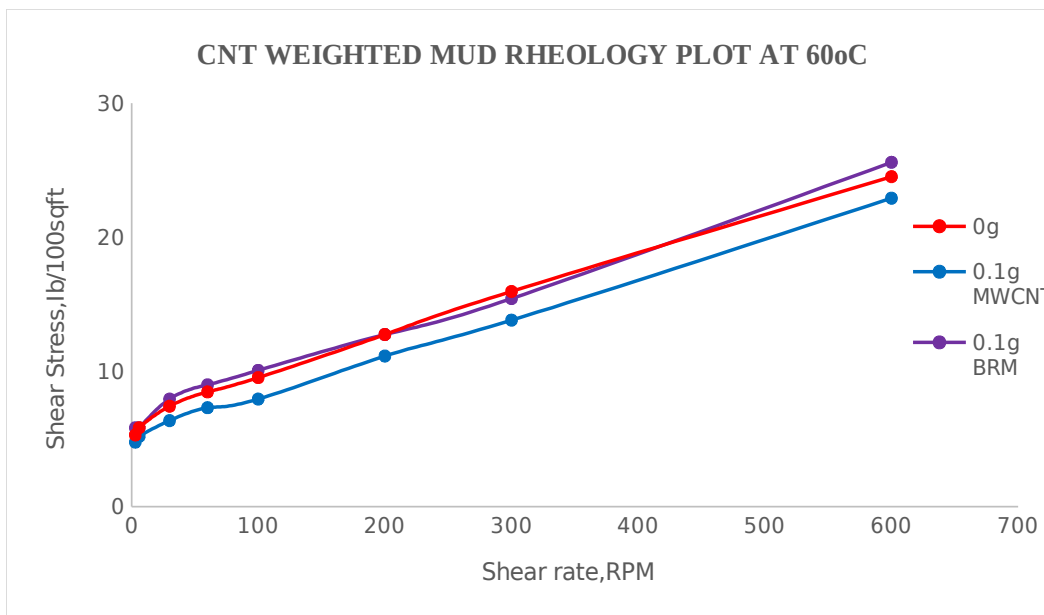


Figure 4.49: Consistency plot for 0.1gMWCNT and 0.1gBRM at 60°C

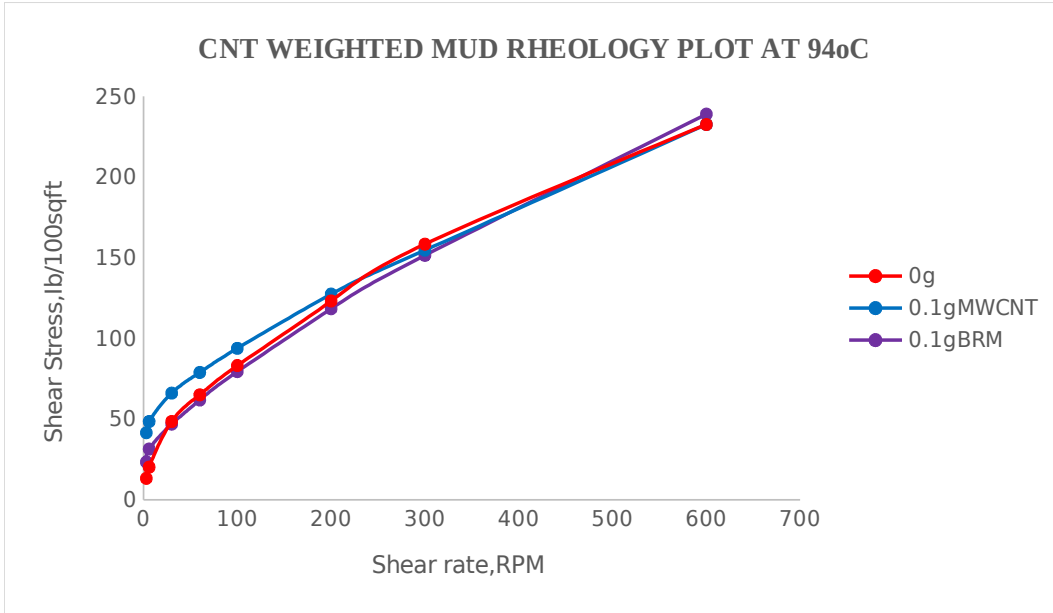


Figure 4.50: Consistency plot for 0.1gMWCNT and 0.1gBRM at 94°C

**MODELS FOR BASE MUD FORMULATION AT 25°C**

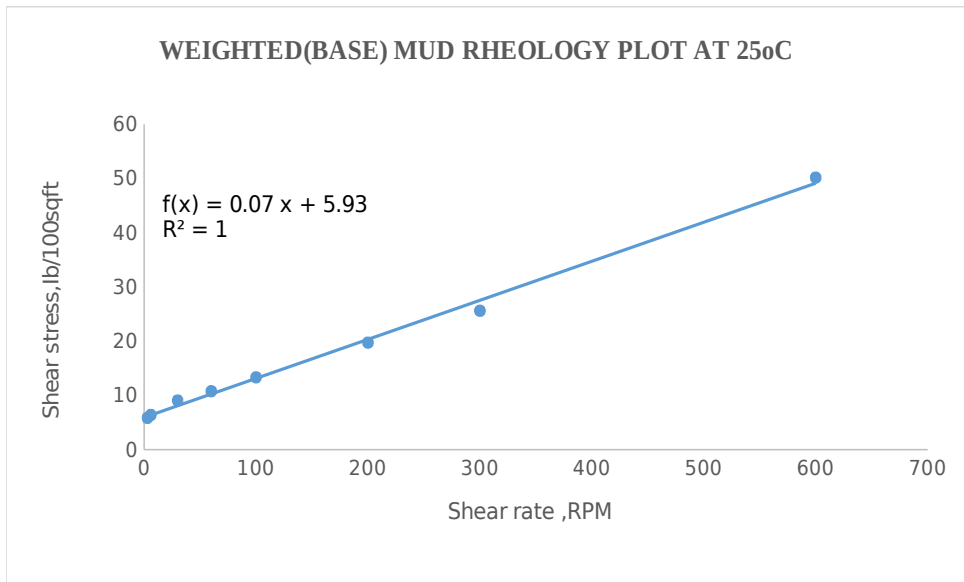


Figure 4.51: Bingham model for Weighted (base) mud rheology plot at 25°C

Figure 4.52: Power law model for Weighted (base) mud rheology plot at 25°C

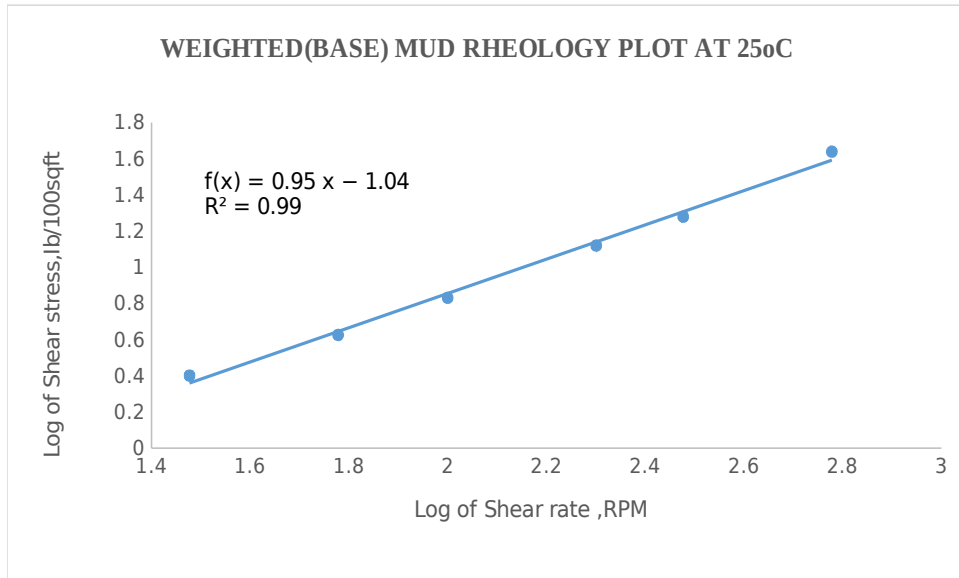


Figure 4.53: Herschel Bulkley model for Weighted (base)mud rheology plot at 25°C

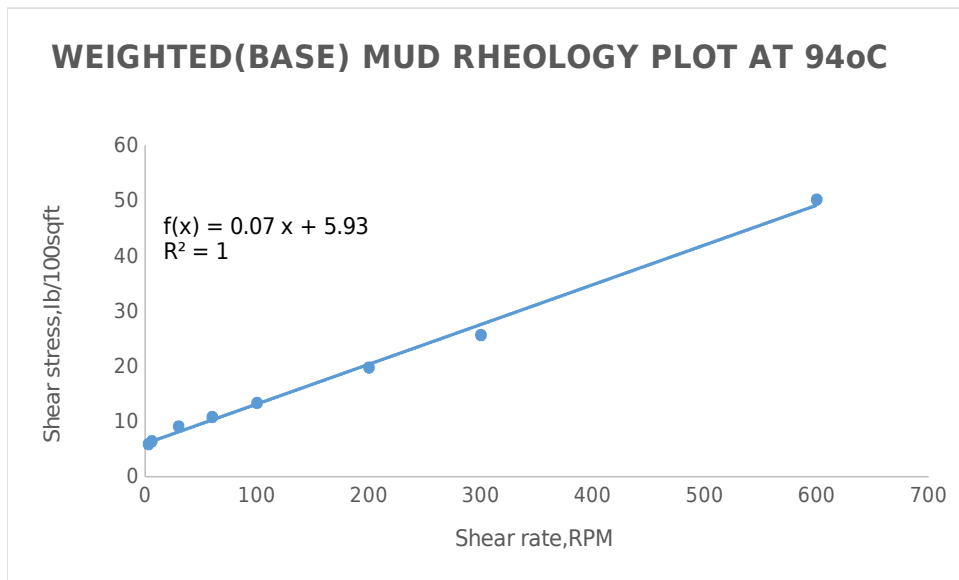


Figure 4.54: Bingham model for Weighted (base)mud rheology plot at 94°C

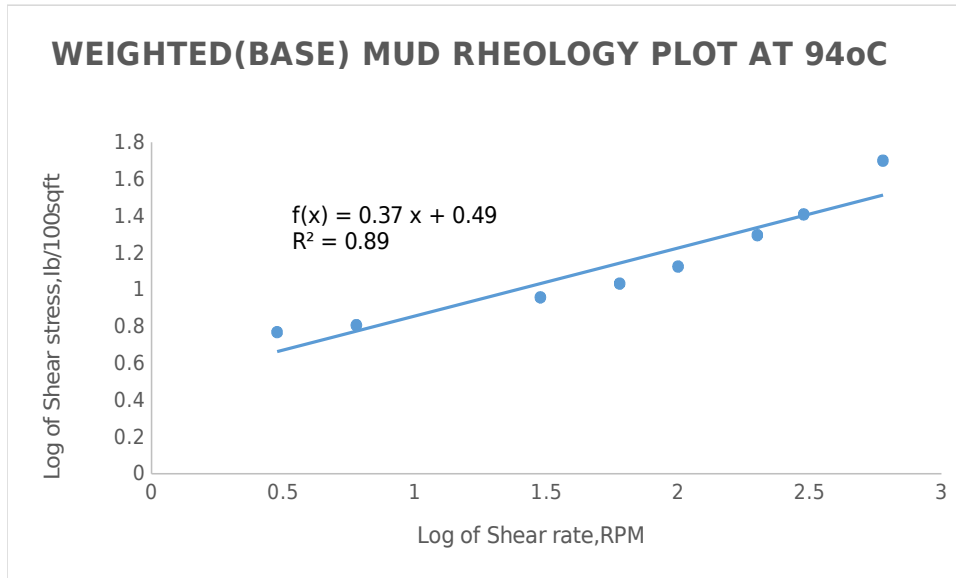


Figure 4.55: Power law model for Weighted (base) mud rheology plot at 94°C

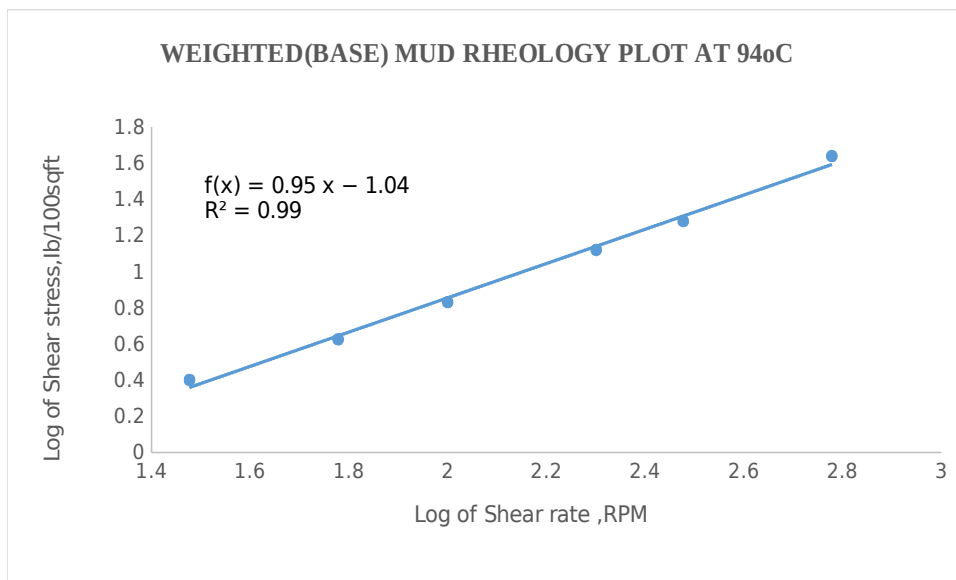


Figure 4.56: Herschel Bulkley model for Weighted (base)mud rheology plot at 94°C

**MODELS FOR MWCNT FORMULATIONS AT 26.5 °C AND 94°C**

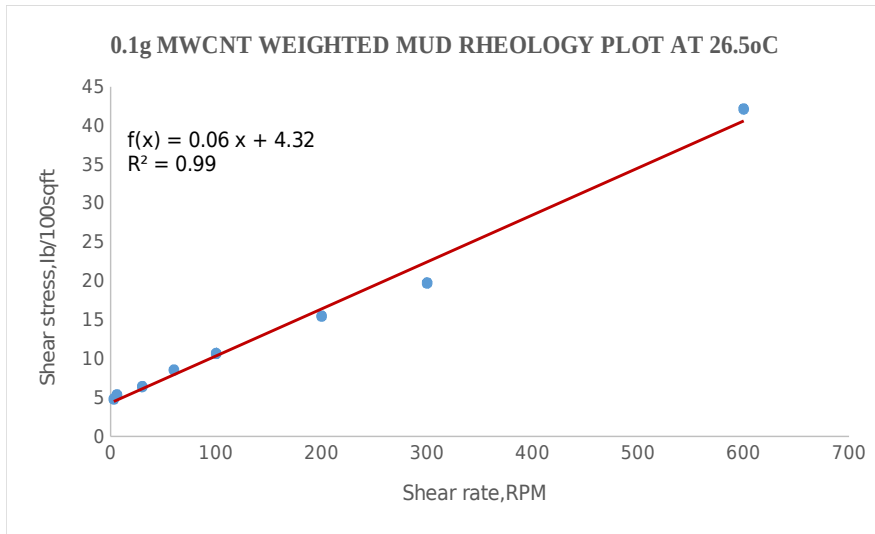


Figure 4.57: Bingham model for MWCNT mud rheology plot at 26.5°C

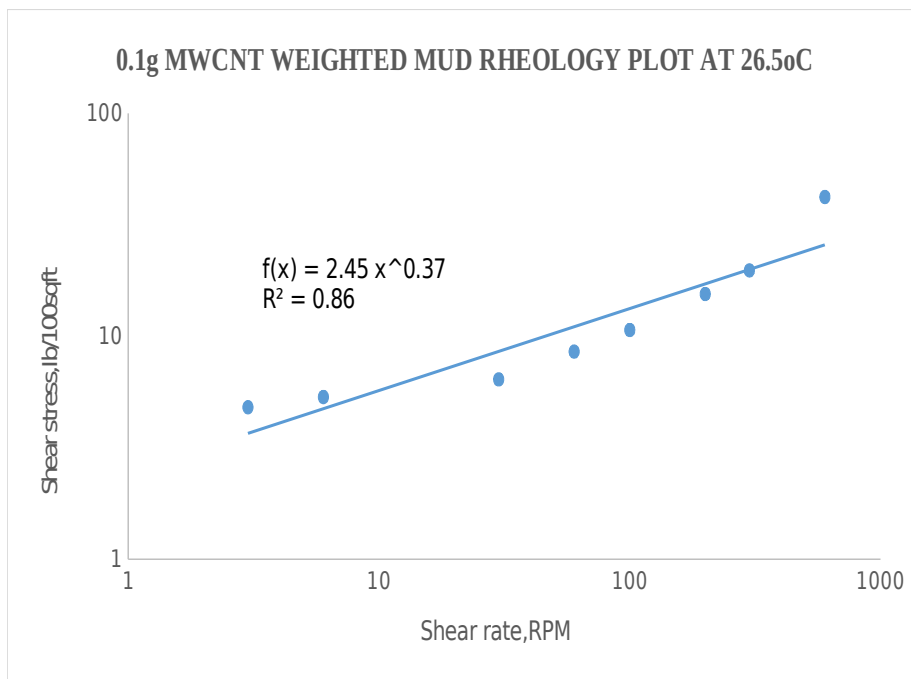


Figure 4.58: Power law model for MWCNT mud rheology plot at 26.5°C

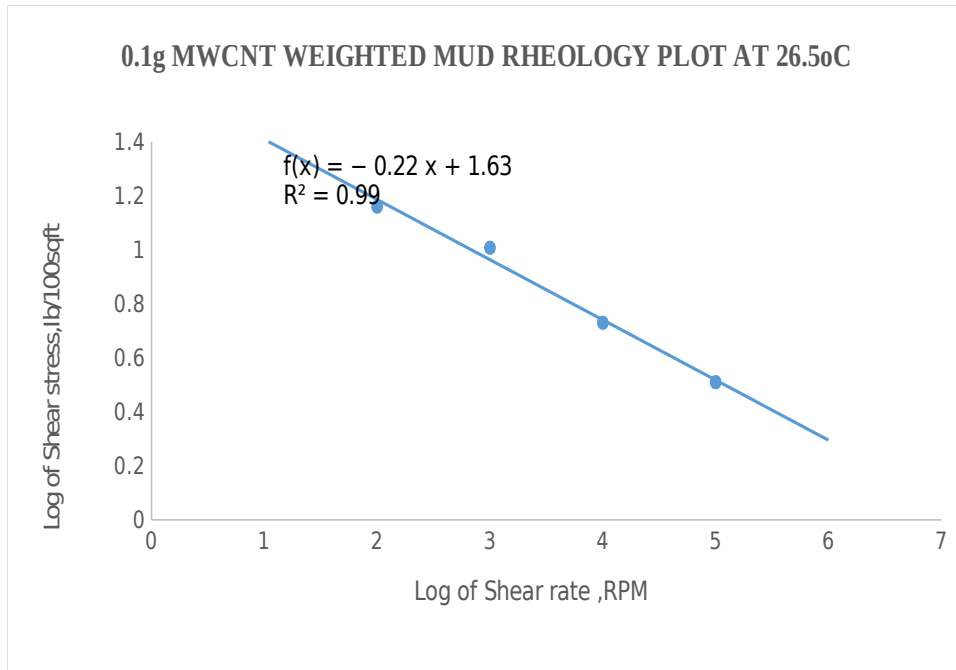


Figure 4.59: Herschel Bulkley model for MWCNT mud rheology plot at 26.5°C

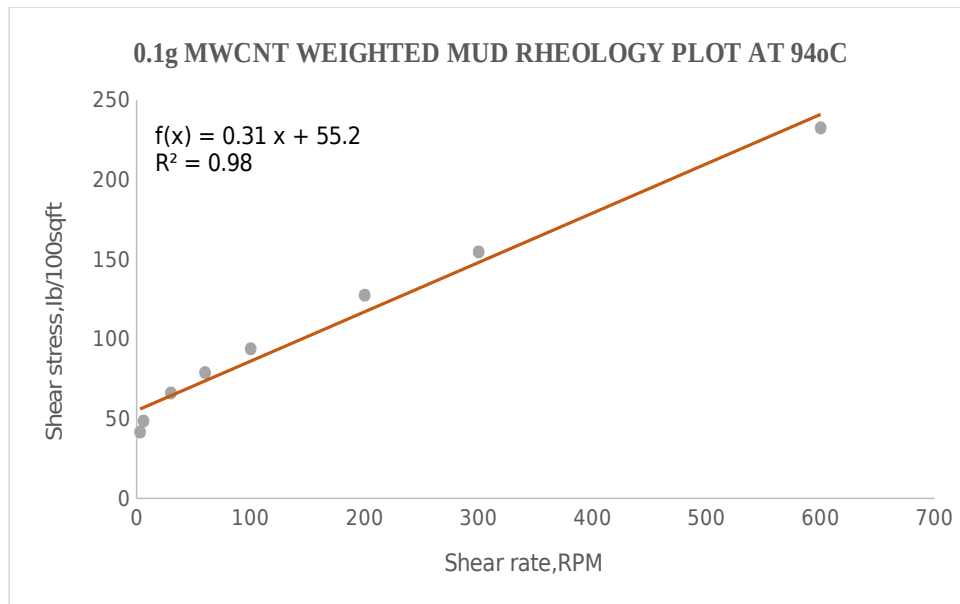


Figure 4.60: Bingham model for MWCNT mud rheology plot at 94°C

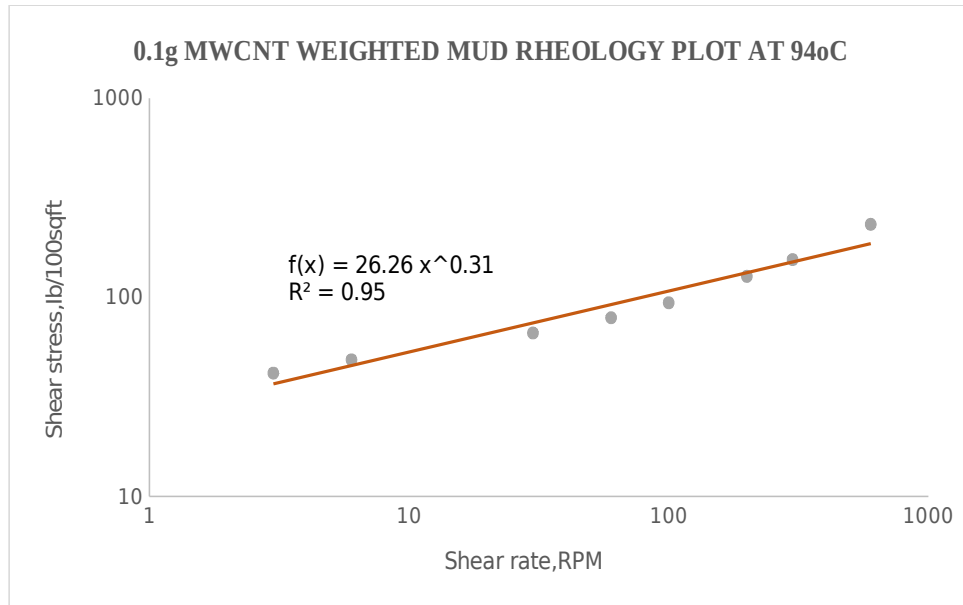


Figure 4.61: Power law model for MWCNT mud rheology plot at 94°C

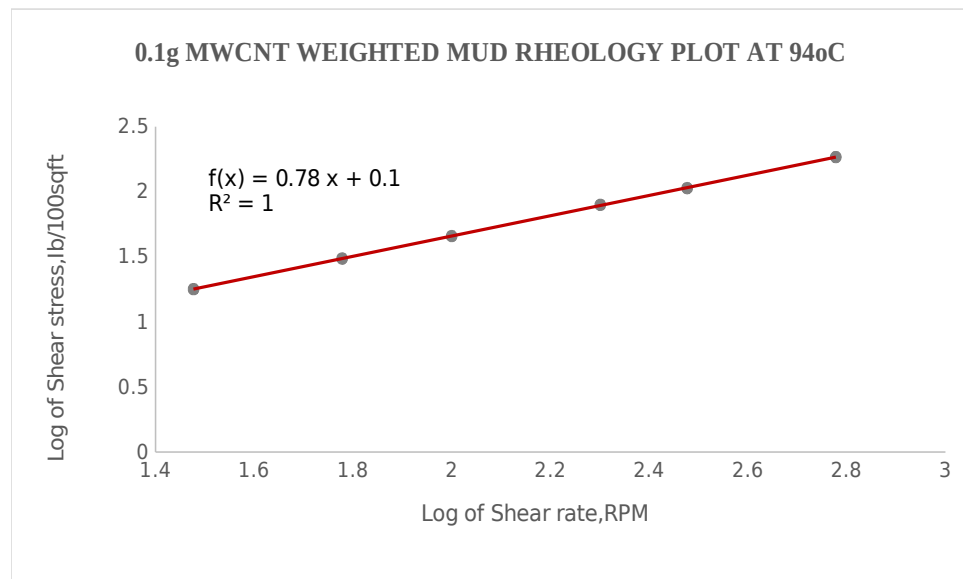


Figure 4.62: Herschel Bulkley model for MWCNT mud rheology plot at 94°C

#### 4.4 Frictional Pressure Losses model estimation

Tables 4.8 and 4.9 show the frictional pressure losses using Herschel Buckley's rheological parameters at 26.5 and 94 °C of base mud (weighted mud without nanoparticles) and MWCNT mud formulations for a conventional pipe configuration for a 10.75 by 9.95 inches and 7.625 by

6.875 inches and 5.5 by 4.892 inches and assumed flow rates of 100gal/min,200 gal/minutes and 300 gal/minutes using Shanghani model.

Table 4.10: Pressure loss model data for base case and MWCNT formulations at 26.5°C

D(inche s)	$K_{base}$	$K_{MWCNT}$	$n_{base}$	$n_{MWCN T}$	Q(gal/ min)	$\Delta Pf/\Delta L$ (Psi/ ft)base	$\Delta Pf/\Delta L$ (Psi/ ft)
4.892	0.091	0.072	0.947 6	0.929 6	100	0.003655635	0.002727261
4.892	0.091	0.072	0.947 6	0.929 6	200	0.007050482	0.005194745
4.892	0.091	0.072	0.947 6	0.929 6	300	0.010353397	0.007572838
6.875	0.091	0.072	0.947 6	0.929 6	100	0.000988672	0.000751271
6.875	0.091	0.072	0.947 6	0.929 6	200	0.001906815	0.001430982
6.875	0.091	0.072	0.947 6	0.929 6	300	0.002800094	0.002086069
9.95	0.091	0.072	0.947 6	0.929 6	100	0.00023883	0.000185141
9.95	0.091	0.072	0.947 6	0.929 6	200	0.000460623	0.000352648
9.95	0.091	0.072	0.947 6	0.929 6	300	0.000676409	0.000514086

Table 4.11: Pressure loss model data for base case and MWCNT formulations at 94°C

D(inche s)	$K_{base}$	$K_{MWCN T}$	$n_{base}$	$n_{MWCN T}$	Q(gal/ min)	$\Delta Pf/\Delta L$ (Psi/ ft)base	$\Delta Pf/\Delta L$ (Psi/ ft)
4.892	2.42 16	1.26 29	0.70 17	0.77 89	100	0.043467979	0.029212 873
4.892	2.42 16	1.26 29	0.70 17	0.77 89	200	0.070697198	0.050124 094
4.892	2.42 16	1.26 29	0.70 17	0.77 89	300	0.093964852	0.068739 127
6.875	2.42 16	1.26 29	0.70 17	0.77 89	100	0.015110559	0.009385 517
6.875	2.42 16	1.26 29	0.70 17	0.77 89	200	0.024576117	0.016103 878
6.875	2.42 16	1.26 29	0.70 17	0.77 89	300	0.032664537	0.022084 519

9.95	2.42 16	1.26 29	0.70 17	0.77 89	100	0.004794635	0.002733 693
9.95	2.42 16	1.26 29	0.70 17	0.77 89	200	0.007798091	0.004690 531
9.95	2.42 16	1.26 29	0.70 17	0.77 89	300	0.010364576	0.006432 496

Pressure losses increase with flowrate for various pipe diameters for base mud and 0.1g MWCNT muds flowing in vertical pipes. The figures 4.40 and 4.41 below are pressure loss versus flowrate plot at 26.5°C and 94°C for base and 0.1g MWCNT mud formulations. It is observed in these plots that as pipe diameter increases from 4.892” to 9.95” in the presence of a constant mud formulation, there is a reduction in pressure loss. The pressure losses appear to be almost constant with diameter 9.95 inches at different flowrates. It also gives information on the effect of MWCNT on pressure losses of the flowing mud. Pressure losses of base mud formulations flowing through pipes of different diameters were higher in comparison to MWCNT mud formulations at room temperature and 94°C

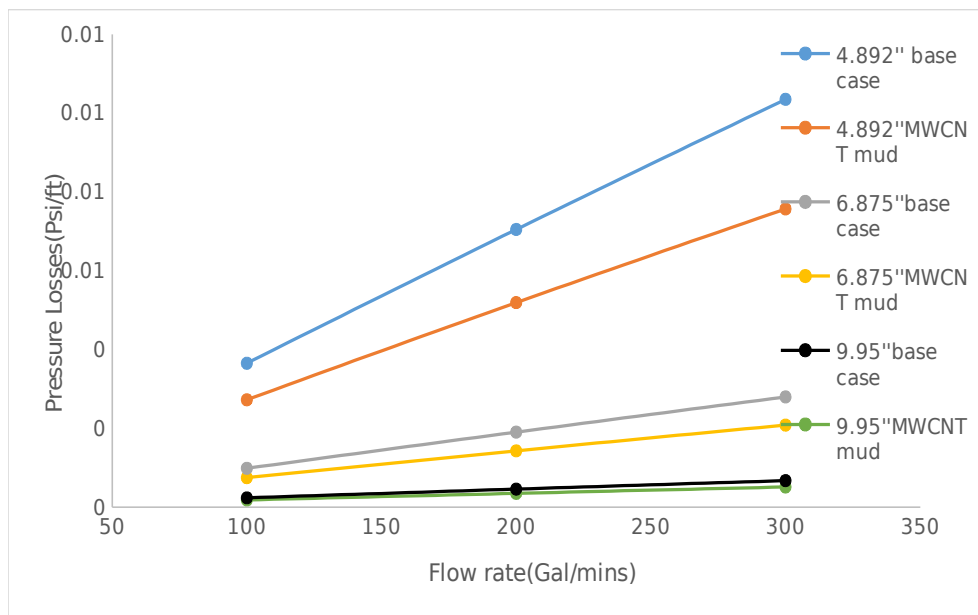


Figure 4.63: Pressure loss profile at 26.5°C for base and 0.1g MWCNT mud formulations

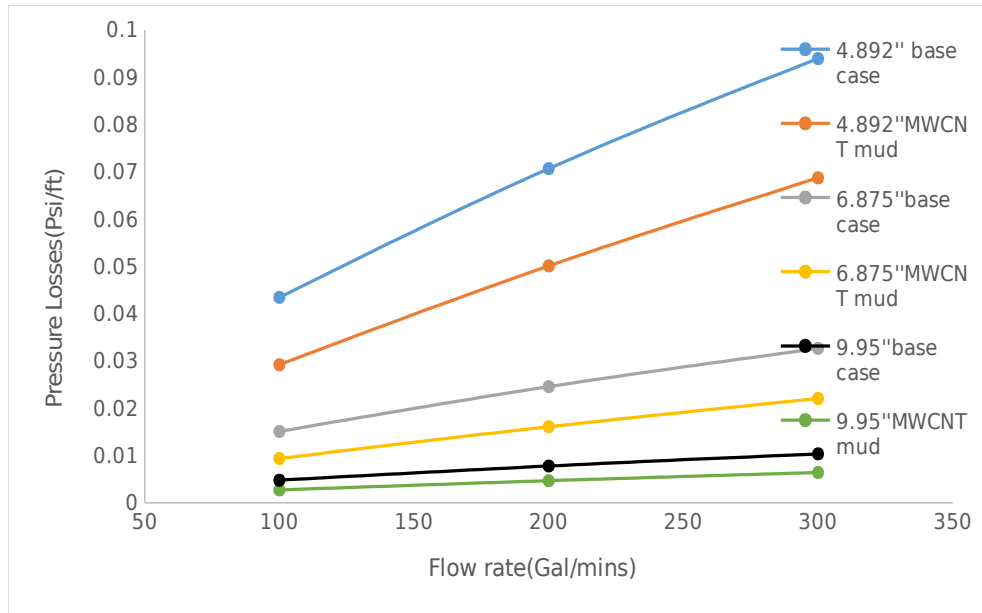


Figure 4.64: Pressure loss profile at 94°C for base and 0.1g MWCNT mud formulations

## CHAPTER 5

### CONCLUSION AND RECOMMENDATION

#### 5.1 Conclusion

This research has attempted to improve gel strength of local biopolymer based Gombe clay and reduce its pressure losses in vertical pipes by addition of Nanoparticles of various sizes.

From the analysis it is concluded that:

- Composites of gum arabic and cassava biopolymers gave better dial reading at 600RPM and plastic viscosity of modified Gombe clay in comparison to formulations having individual polymers of corn starch, cassava starch and gum arabic. Gel readings were still below API standards.

- MWCNT and BRM formulations had little or no significant effect on gel strength at room temperature but gave better gel strength at high temperature in comparison to mud formulations having no CNT.
- At 94°C, optimum amount of CNTs required to improve gel strength lies between the range of 0.1 and 0.2g.MWCNTs quantity beyond 0.2g behaves as a thinner in modified Gombe clay formulations.
- Herschel-bulkley models were most appropriate to describe MWCNT formulations in comparison to Bingham and Power law models based on regression's plot  $R^2$  values
- 0.1g MWCNT reduce pressure losses of base mud formulation flowing through vertical pipes by a minimum and maximum of 22% and 43% approximately at 26°C and 94°C.

## 5.2 Recommendations

The following recommendations are made for further study.

- Development of new mud formulations involving indigenous biopolymers and BRM/MWCNT to improve gel strength at both room and high temperature using Response surface methodology, Genetic algorithm ,Golden section and Linear Programming to determine the best optimisation technique.
- Hydraulics and simulation of cutting carrying capacity of the developed mud which involves Model development, Pressure loss estimation ,Cutting transport efficiency determination and Hydraulics optimization study using Response Surface Methodology and other optimisation techniques.

## REFERENCES

- (SPE textbook series 2) Jr. Adam T. Bourgoyne, Keith K. Millheim, Martin E. Chenevert, Jr. F. S. Young-*Applied Drilling Engineering-Society of Petroleum Engineers (1986)\_2.pdf*. (n.d.).
- Alflah, S., Balola, A. A., Ibrahim, A. A., & Wagialla, A. H. (2015). Effects of Gum Arabic Addition on the Behaviour of Water Base Drilling Fluids. *SUST Journal of Engineering*

*and Computer Science (JECS), 16(3), 1–8.*

Arinkoola, A O, Salawudeen, T. O., Salam, K. K., Jimoh, M. O., Abidemi, G. O., & Atitebi, Z. M. (2019). *Optimization of Water - Based Drilling Fluid Produced Using Modified Nigerian Bentonite and Natural Biopolymers : Reduced Experiment and Response Surface Methodology.* 16(1), 39–53.

Arinkoola, Akeem Olatunde, Olalekan, S. T., Salam, K. K., Omolola, J. M., & Gafar, A. O. (2018). *Potential Evaluation and Optimization of Natural Biopolymers in Water-Based Drilling Mud.* 52(June), 1–12. <https://doi.org/10.22059/jchpe.2018.233480.1197>

Bahrainian, S. S., Nabati, A., & Hajidavalloo, E. (2018). *Improved Rheological Model of Oil-Based Drilling Fluid for South- western Iranian Oilfields.* 8(3), 53–71. <https://doi.org/10.22078/jpst.2017.2706.1459>

Caenn, R., Darley†, H. C. H., & Gray†, G. R. (2016). The Rheology of Drilling Fluids. In *Composition and Properties of Drilling and Completion Fluids.* <https://doi.org/10.1016/b978-0-12-804751-4.00006-7>

Clark, P. (2007). *Drilling Mud Rheology and the API Recommended Measurements.* 933–941. <https://doi.org/10.2523/29543-ms>

de Assis, C. A., Iglesias, M. C., Bilodeau, M., Johnson, D., Phillips, R., Peresin, M. S., ... Gonzalez, R. (2018). Cellulose micro- and nanofibrils (CMNF) manufacturing - financial and risk assessment. *Biofuels, Bioproducts and Biorefining*, 12(2), 251–264. <https://doi.org/10.1002/bbb.1835>

de Souza Mendes, P. R., & Thompson, R. L. (2019). Time-dependent yield stress materials. *Current Opinion in Colloid and Interface Science*, 43(March), 15–25. <https://doi.org/10.1016/j.cocis.2019.01.018>

*Faculty of Science and Technology MASTER ' S THESIS.* (2015).

Gbadamosi, A. O., Junin, R., Oseh, J. O., Agi, A., Yekeen, N., Abdalla, Y., ... Yusuff, A. S. (2018). *Improving Hole Cleaning Efficiency using Nanosilica in Water-Based Drilling Mud.* <https://doi.org/10.2118/193401-ms>

- Ghazali, N. A., Alias, N. H., Mohd, T. A. T., Adeib, S. I., & Noorsuhana, M. Y. (2015). Potential of Corn Starch as Fluid Loss Control Agent in Drilling Mud. *Applied Mechanics and Materials*, 754–755(September), 682–687.  
<https://doi.org/10.4028/www.scientific.net/amm.754-755.682>
- Guo, B., & Liu, G. (2011). Mud Hydraulics Fundamentals. In *Applied Drilling Circulation Systems*. <https://doi.org/10.1016/b978-0-12-381957-4.00002-4>
- Halliburton, J. M. (2007). *Thixotropy and Yield Stress Behavior in Drilling Fluids*. (April 2007). Retrieved from <https://www.researchgate.net/publication/255771583>
- Hossain, M. E. (2016). Fundamentals of Drilling Engineering. In *Fundamentals of Drilling Engineering* (Vol. 12). <https://doi.org/10.1002/9781119083931>
- Jr, C. E. W., Bruce, G. H., Oil, H., & Co, R. (1951). *CARRYING CAPACITY OF DRILLING MUDS Power Savings by Reduction of Annular Velocities*. 192.
- Kazemi-Beydokhti, A., & Hajiabadi, S. H. (2018). Rheological investigation of smart polymer/carbon nanotube complex on properties of water-based drilling fluids. *Colloids and Surfaces A: Physicochemical and Engineering Aspects*, 556(June), 23–29.  
<https://doi.org/10.1016/j.colsurfa.2018.07.058>
- Nguyen, Q.-H., & Nguye, N.-D. (2012). Incompressible Non-Newtonian Fluid Flows. *Continuum Mechanics - Progress in Fundamentals and Engineering Applications*.  
<https://doi.org/10.5772/26091>
- Ogunmola, E. O., Arinkoola, A. O., Salam, K. K., Jimoh, M. O., & Salawudeen, T. O. (2017). Effect of inert fibre on performance of B. eurycoma as rheology and filtration control additive in water-based drilling fluid. *International Journal of Petroleum Engineering*, 2(3), 191. <https://doi.org/10.1504/ijpe.2016.10002637>
- Olise, O. S., Ekaette, N., & Okologume, W. (2017). Effect of Aging on Water Based Mud. *International Journal of Engineering and Modern Technology*, 3(5), 26–38.
- Pivnicka, S., Nguyen, T. C., Al-safran, E., & Saasen, A. (2015). Journal of Petroleum Science and Engineering Pressure gradient prediction of time-dependent drilling fluids and the effect of acceleration. *Journal of Petroleum Science and Engineering*, 135, 246–252.

<https://doi.org/10.1016/j.petrol.2015.09.008>

- Sami, N. A. (2016). Effect of magnesium salt contamination on the behavior of drilling fluids. *Egyptian Journal of Petroleum*, 25(4), 453–458. <https://doi.org/10.1016/j.ejpe.2015.10.011>
- Saxena, A., Pathak, A. K., Ojha, K., & Sharma, S. (2017). Experimental and modeling hydraulic studies of foam drilling fluid flowing through vertical smooth pipes. *Egyptian Journal of Petroleum*, 26(2), 279–290. <https://doi.org/10.1016/j.ejpe.2016.04.006>
- Taiwo, A., Joel, O. F., & Kazeem, A. A. (2011). Investigation of local polymer (Cassava starches) as a substitute for imported sample in viscosity and fluid loss control of water based drilling mud. *Journal of Engineering and Applied Sciences*, 6(12), 43–48.
- Zamora, M., & Power, D. (2002). Making a Case for AADE Hydraulics and the Unified Rheological Model. *Drilling & Completion Fluids and Waste Management*, 1–8.
- Bloys, B., Davis, N., Smolen, B., Bailey, L., Reid, P., Fraser, L. and Hodder, M., “Designing and managing drilling fluids”, *Oilfield*, 6, 33 (1994). ([http://www.slb.com/~media/Files/resources/oilfield\\_review/ors94/0494/p33\\_43.pdf](http://www.slb.com/~media/Files/resources/oilfield_review/ors94/0494/p33_43.pdf)).
- Annis, M. R. and Smith, M. V., *Drilling fluid technology*, Exxon Company, USA, (1974).
- Baba Hamed, S. and Belhadri, M., “Rheological properties of biopolymers drilling fluids”, *Petroleum Sci. Eng.*, 67 (3), 84 (2009).
- Teleman, A., Nordström, N., Tenkanen, M., et al., “Isolation and characterization of O-acetylated glucomannans from aspen and birch wood”, *Carbohydr. Res.*, 338, 525 (2003).